Electronic Supplementary Material (ESI) for Journal of Materials Chemistry C.

Magnetocaloric *Ln*(HCO_2)(C_2O_4) frameworks: Synthesis, Structure and Magnetic Properties

Mario Falsaperna,[a] Gavin B.G. Stenning,[b] Ivan da Silva,[b] and Paul J. Saines*[a]

[a]School of Phyisical Sciences, Ingram Building, University of Kent, Canterbury, CT2 7NH

[b]ISIS Facility, STFC Rutherford Appleton Laboratory, Chilton, Didcot, OX11 0QX, UK

* Corresponding Author Email: P.Saines@kent.ac.uk

Electronic Supplementary Information (ESI)

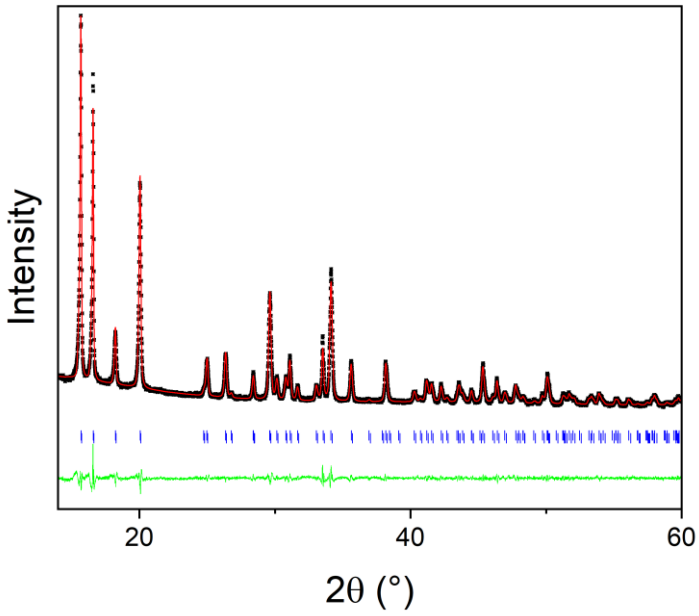

Fig. S1: Conventional powder X-ray diffraction pattern of $Sm(HCO_2)(C_2O_4)$ fitted using the Le Bail method to highlight phase purity. The crosses, red and green lines are experimental and calculated intensities and the difference curve. Vertical markers indicate the position of the Bragg reflections. R_p, R_{wp} and χ^2 of 2.88 %, 3.66 % and 3.33 are obtained respectively from the refinement with a = 7.13136(14) Å, b = 10.6840(2) Å and c = 6.65763(15) Å for the unit cell parameters.

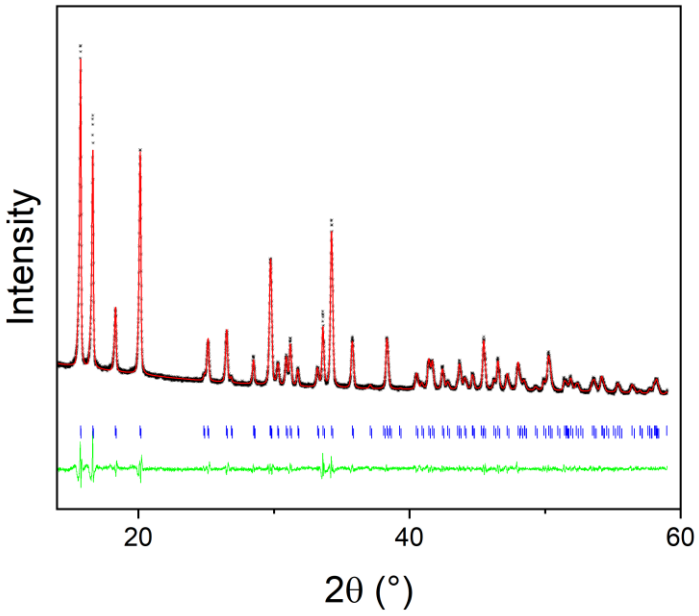

Fig. S2: Conventional powder X-ray diffraction pattern of $Eu(HCO_2)(C_2O_4)$ fitted using the Le Bail method to highlight phase purity. The crosses, red and green lines are experimental and calculated intensities and the difference curve. Vertical markers indicate the position of the Bragg reflections. R_p, R_{wp} and χ^2 of 2.66 %, 3.47 % and 3.62 are obtained respectively from the refinement with a = 7.08694(14) Å, b = 10.6524(2) Å and c = 6.6324(2) Å for the unit cell parameters.

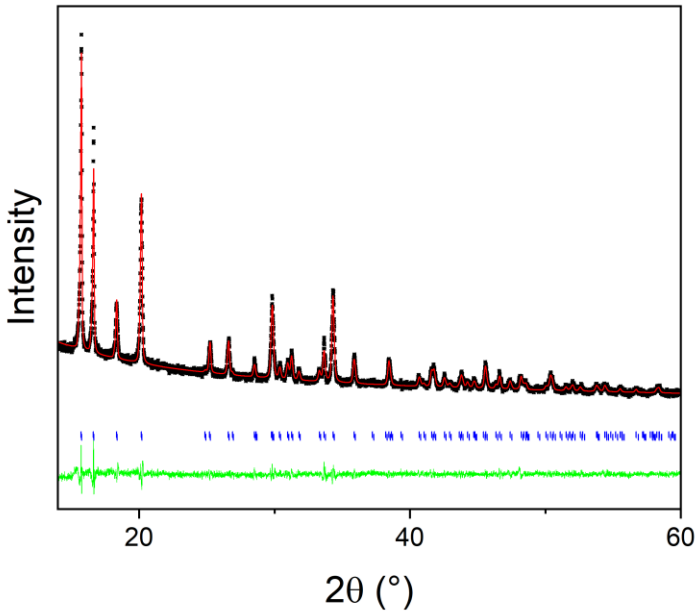

Fig. S3: Conventional powder X-ray diffraction pattern of $Gd(HCO_2)(C_2O_4)$ fitted using the Le Bail method to highlight phase purity. The crosses, red and green lines are experimental and calculated intensities and the difference curve. Vertical markers indicate the position of the Bragg reflections. R_p, R_{wp} and χ^2 of 3.03 %, 3.82 % and 1.81 are obtained respectively from the refinement with a = 7.0431(3) Å, b = 10.6194(4) Å and c = 6.6070(3) Å for the unit cell parameters.

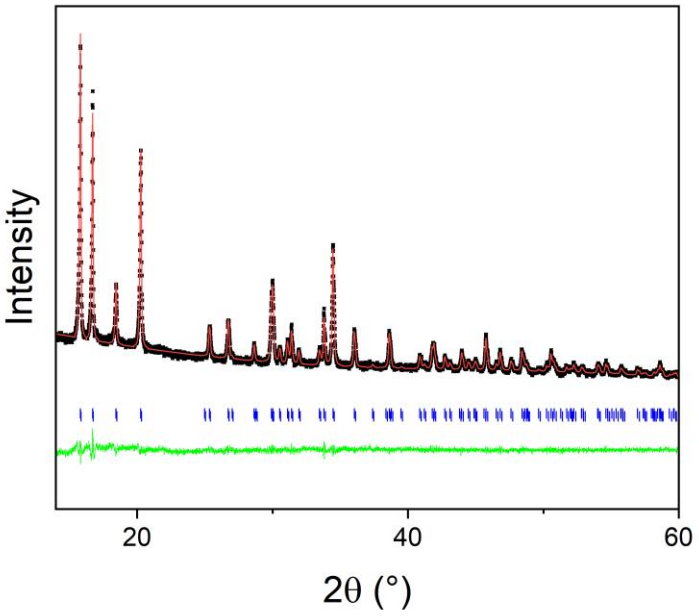

Fig. S4: Conventional powder X-ray diffraction pattern of $Tb(HCO_2)(C_2O_4)$ fitted using the Le Bail method to highlight phase purity. The crosses, red and green lines are experimental and calculated intensities and the difference curve. Vertical markers indicate the position of the Bragg reflections. R_p, R_{wp} and χ^2 of 2.30 %, 3.65 % and 1.72 are obtained respectively from the refinement with a = 7.02274(18) Å, b = 10.5980(3) Å and c = 6.59748(18) Å for the unit cell parameters.

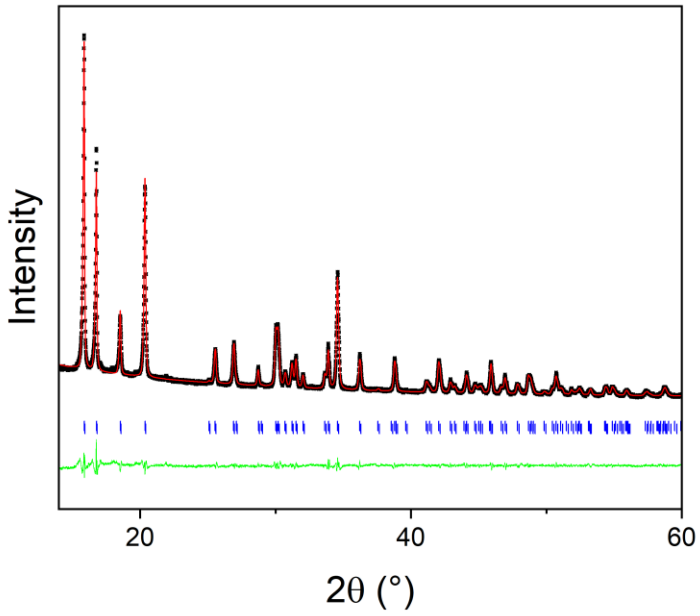

Fig. S5: Conventional powder X-ray diffraction pattern of $Dy(HCO_2)(C_2O_4)$ fitted using the Le Bail method to highlight phase purity. The crosses, red and green lines are experimental and calculated intensities and the difference curve. Vertical markers indicate the position of the Bragg reflections. R_p, R_{wp} and χ^2 of 2.56 %, 3.23 % and 3.52 are obtained respectively from the refinement with a = 6.98194(13) Å, b = 10.5752(2) Å and c = 6.58162(14) Å for the unit cell parameters.

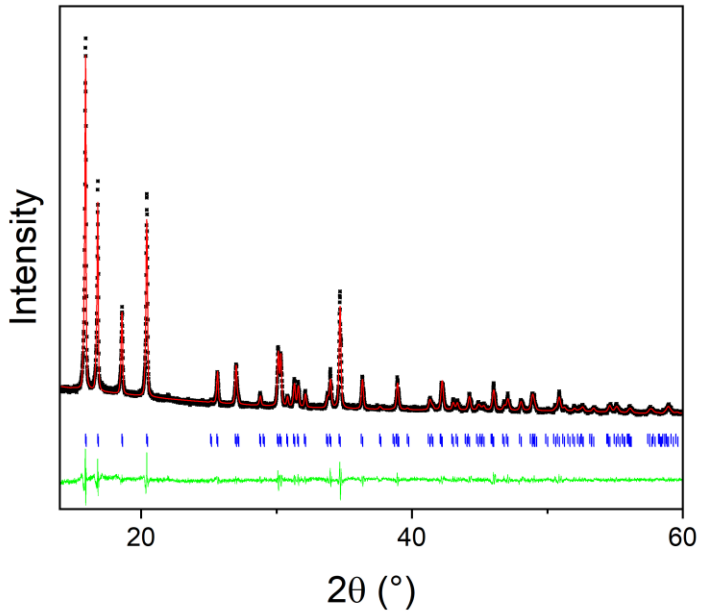

Fig. S6: Conventional powder X-ray diffraction pattern of $Ho(HCO_2)(C_2O_4)$ fitted using the Le Bail method to highlight phase purity. The crosses, red and green lines are experimental and calculated intensities and the difference curve. Vertical markers indicate the position of the Bragg reflections. R_p, R_{wp} and χ^2 of 4.09 %, 5.13 % and 2.84 are obtained respectively from the refinement with a = 6.97292(19) Å, b = 10.5811(4) Å and c = 6.58207(20) Å for the unit cell parameters.

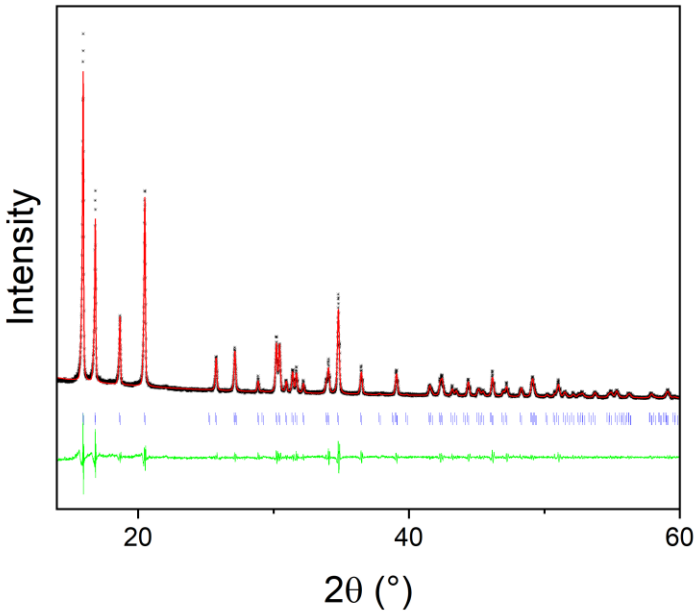

Fig. S7: Conventional powder X-ray diffraction pattern of $Er(HCO_2)(C_2O_4)$ fitted using the Le Bail method to highlight phase purity The crosses, red and green lines are experimental and calculated intensities and the difference curve. Vertical markers indicate the position of the Bragg reflections. R_p, R_{wp} and χ^2 of 4.36 %, 5.58 % and 4.63 are obtained respectively from the refinement with a = 6.92593(17) Å, b = 10.5448(3) Å and c = 6.55559(18) Å for the unit cell parameters.

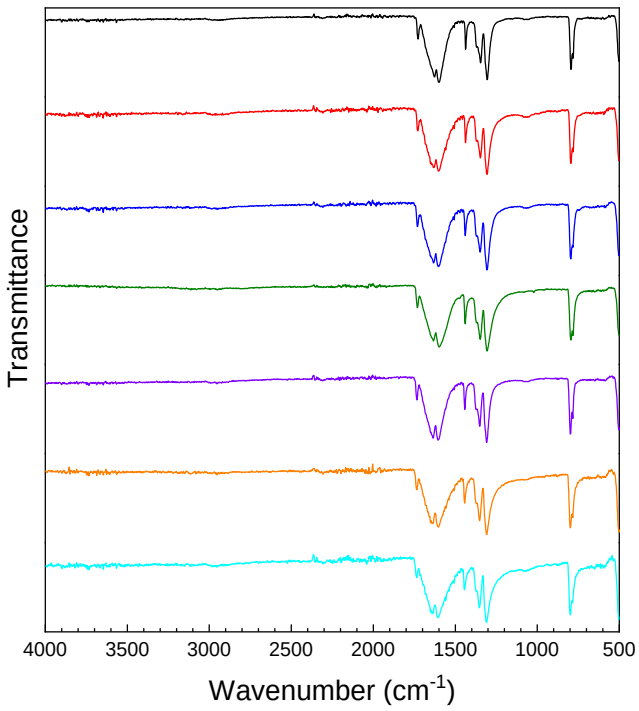

Fig. S8: Fourier transform infrared spectra of $Ln(HCO_2)(C_2O_4)$ (*Ln* = Sm – Er from top to bottom). A band at 1735 cm^{-1} is ascribable to the stretching of a shortened C-O bond length, confirmed by the presence of a bands at 1632, 1601 and 1305 cm^{-1} similarly attributable to the stretching of C-O. Band at 1367 and 1345 cm^{-1} are an indication of C-H bending modes, confirming the presence of the formate ligand in the structure.

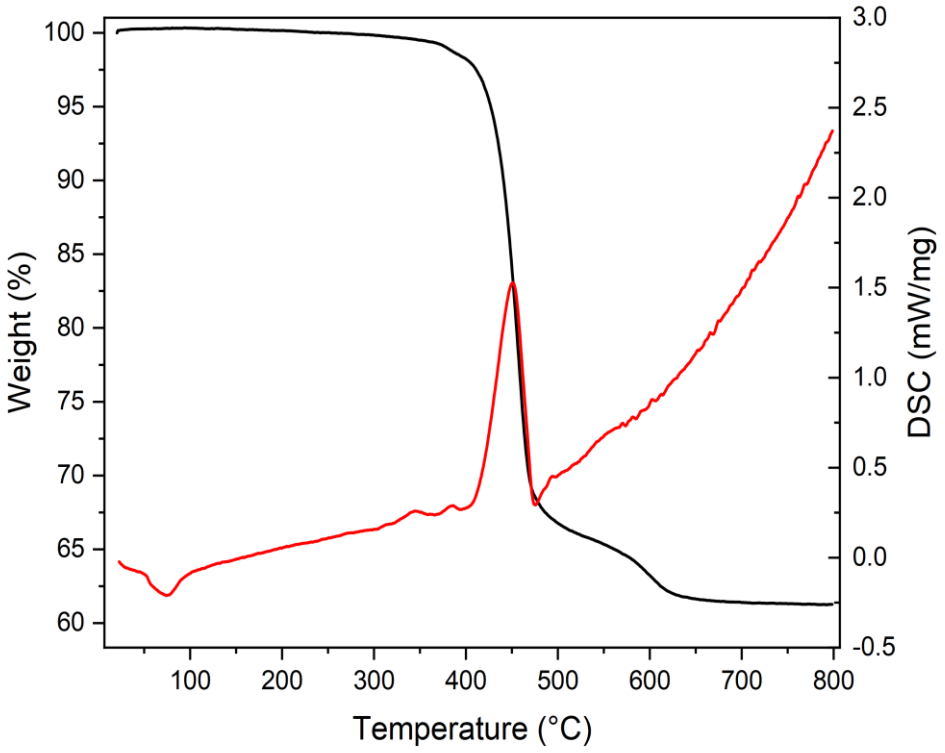

Fig. S9: Thermogravimetric analysis for $Sm(HCO_2)(C_2O_4)$ showing weight loss and differential curves at a heating rate of 10 ^{o}C/min from 24 to 800 ^{o}C.

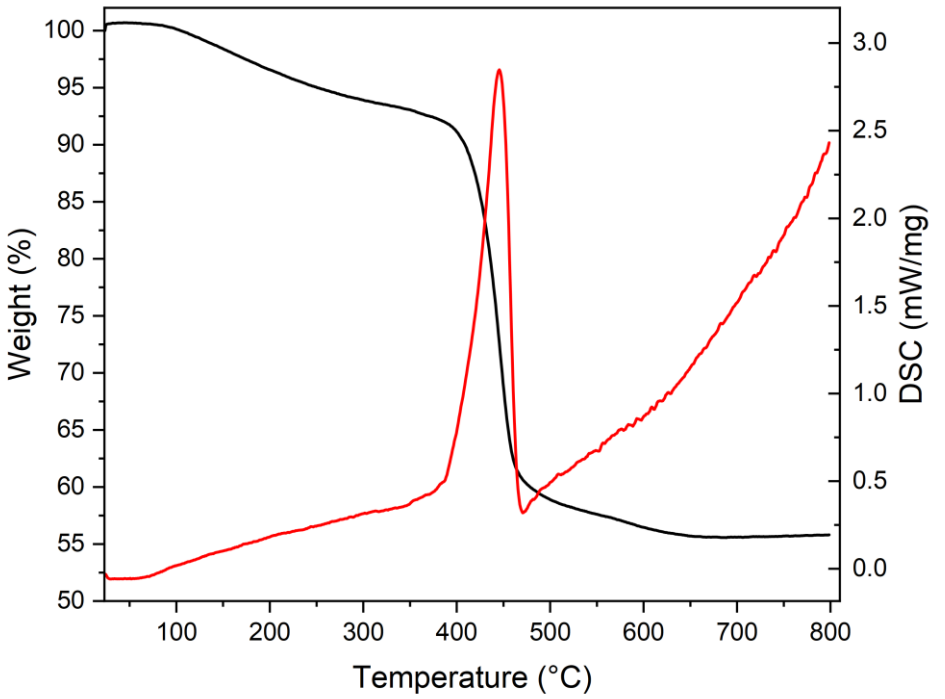

Fig. S10: Thermogravimetric analysis for $Eu(HCO_2)(C_2O_4)$ showing weight loss and differential curves at a heating rate of 10 ^{o}C/min from 24 to 800 ^{o}C.

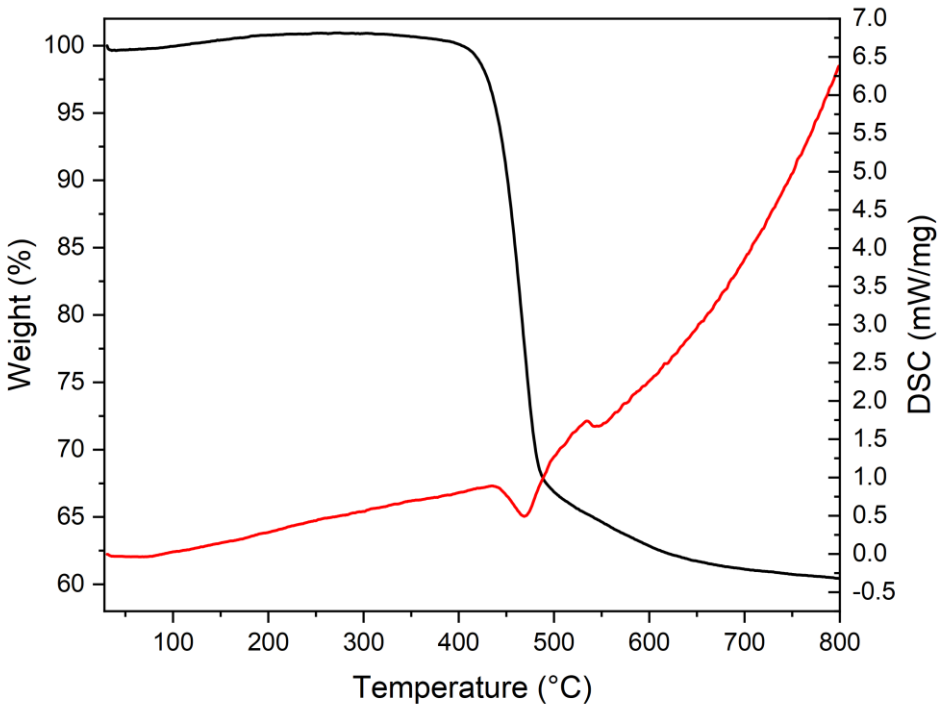

Fig. S11: Thermogravimetric analysis for $Gd(HCO_2)(C_2O_4)$ showing weight loss and differential curves at a heating rate of 10 ^oC/min from 24 to 800 ^oC.

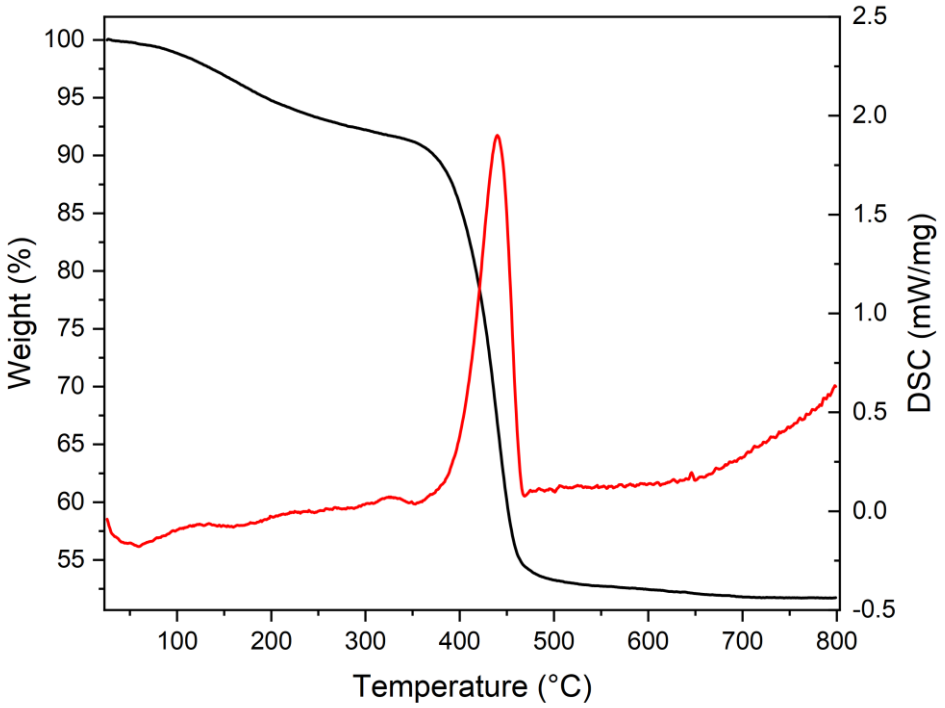

Fig. S12: Thermogravimetric analysis for $Tb(HCO_2)(C_2O_4)$ showing weight loss and differential curves at a heating rate of 10 ^oC/min from 24 to 800 ^oC.

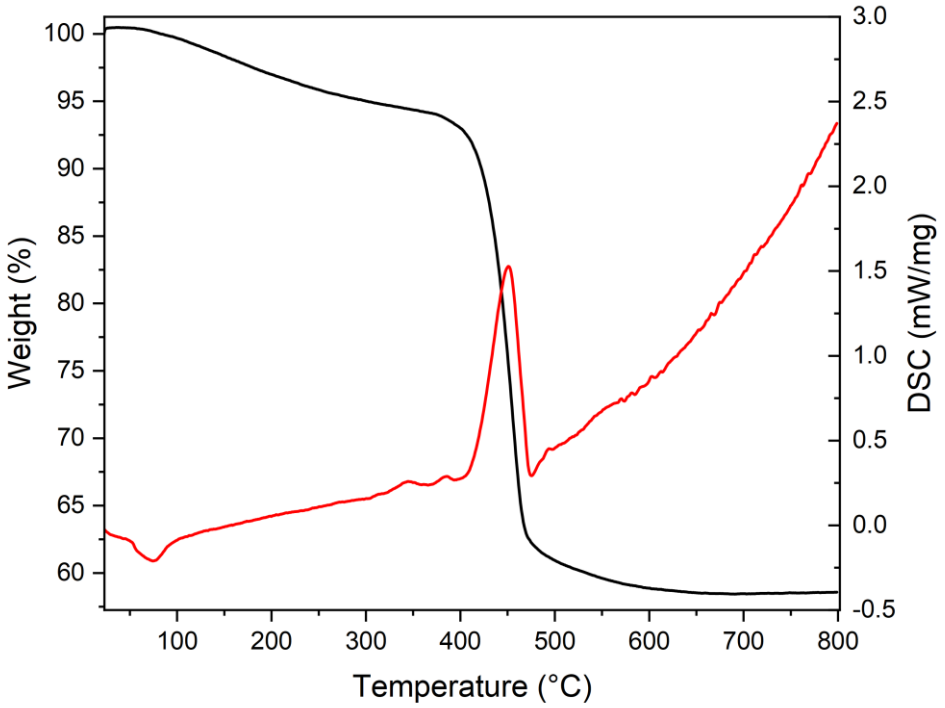

Fig. S13: Thermogravimetric analysis for $Dy(HCO_2)(C_2O_4)$ showing weight loss and differential curves at a heating rate of 10 ^oC/min from 24 to 800 ^oC.

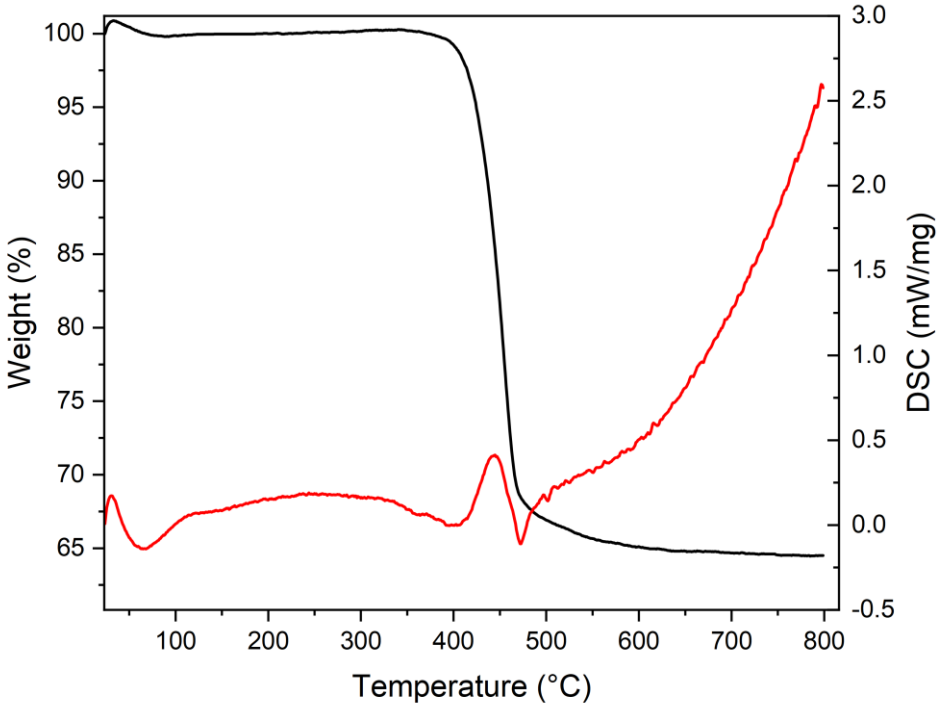

Fig. S14: Thermogravimetric analysis of $Ho(HCO_2)(C_2O_4)$ showing weight loss and differential curves at a heating rate of 10 ^oC/min from 24 to 800 ^oC.

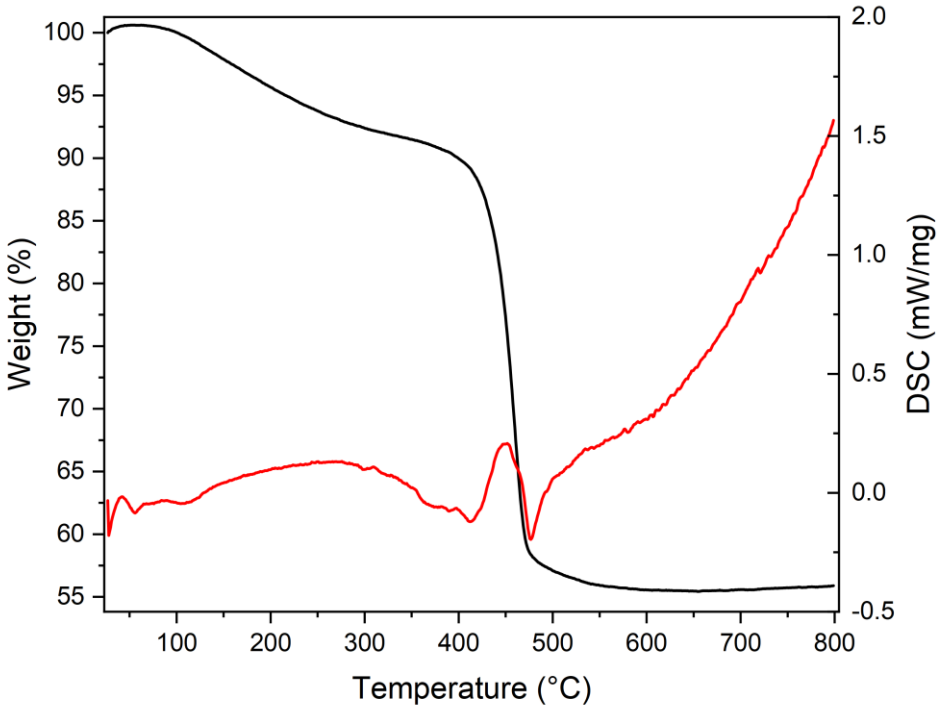

Fig. S15: Thermogravimetric analysis for $Er(HCO_2)(C_2O_4)$ showing weight loss and differential curves at a heating rate of 10 ^oC/min from 24 to 800 ^oC.

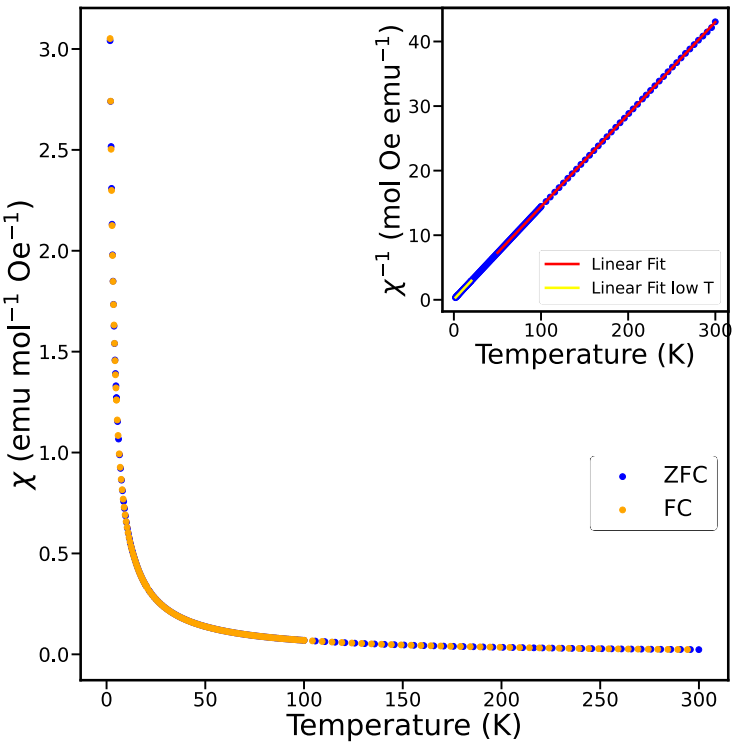

Fig. S16: ZFC and FC susceptibility measurements for $Gd(HCO_2)(C_2O_4)$ in a 0.1 T field. The insert shows the inverse susceptibility and the low and high temperature Curie-Weiss fits to the data obtained between 2-20 K and 50–300 K, respectively.

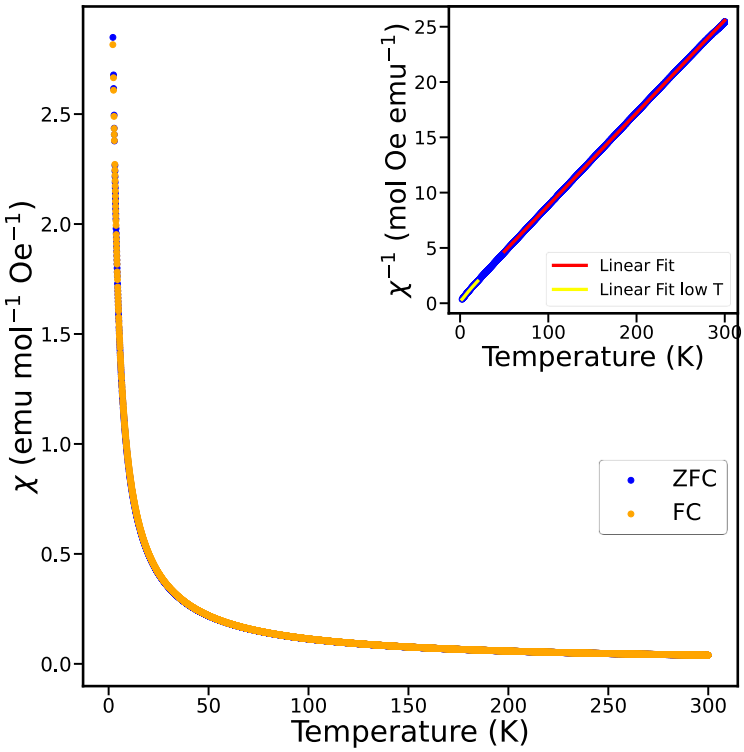

Fig. S17: ZFC and FC susceptibility measurements for $Tb(HCO_2)(C_2O_4)$ in a 0.1 T field. The insert shows the inverse susceptibility and the low and high temperature Curie-Weiss fits to the data obtained between 2-20 K and 50–300 K, respectively.

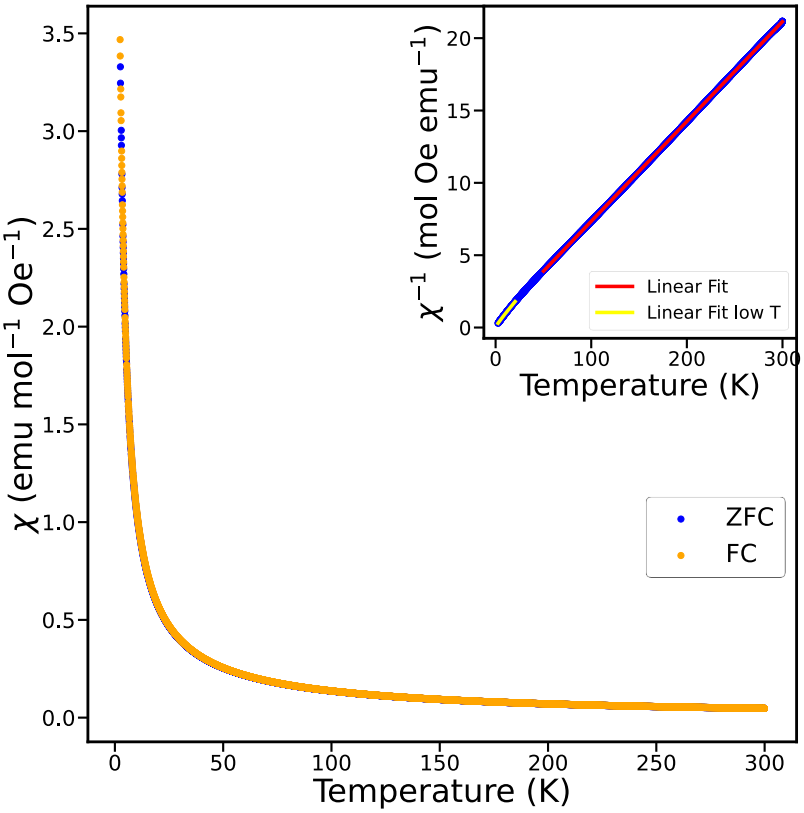

Fig. S18: ZFC and FC susceptibility measurements for $Dy(HCO_2)(C_2O_4)$ in a 0.1 T field. The insert shows the inverse susceptibility and the low and high temperature Curie-Weiss fits to the data obtained between 2-20 K and 50–300 K, respectively.

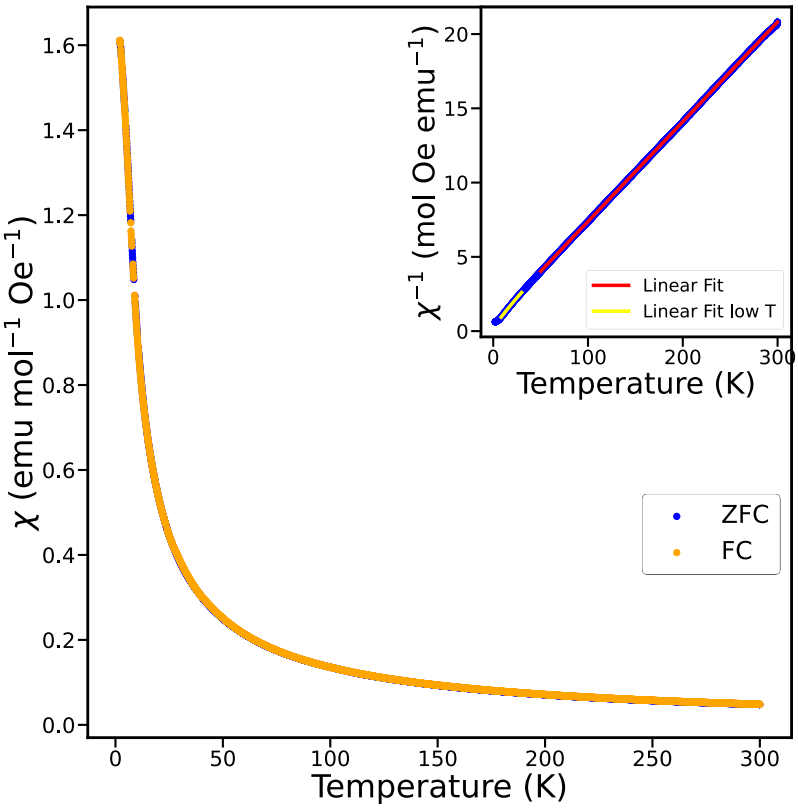

Fig. S19: ZFC and FC susceptibility measurements for $Ho(HCO_2)(C_2O_4)$ in a 0.1 T field. The insert shows the inverse susceptibility and the low and high temperature Curie-Weiss fits to the data obtained between 8-20 K and 50–300 K, respectively.

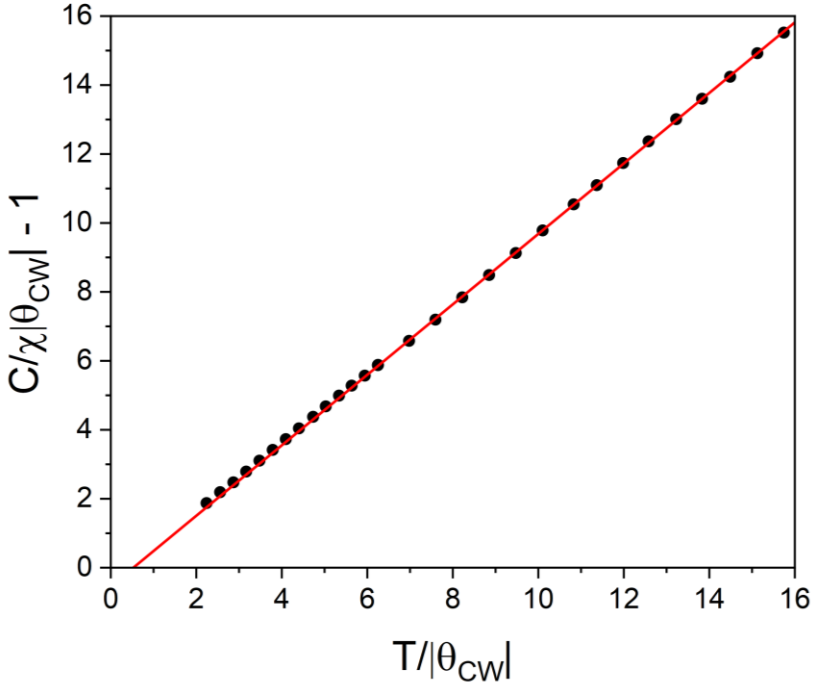

Fig. S20: Plot of $C/\chi|\theta_{CW}| - 1$ as a function of $T/|\theta_{CW}|$ for $Gd(HCO_2)(C_2O_4)$.

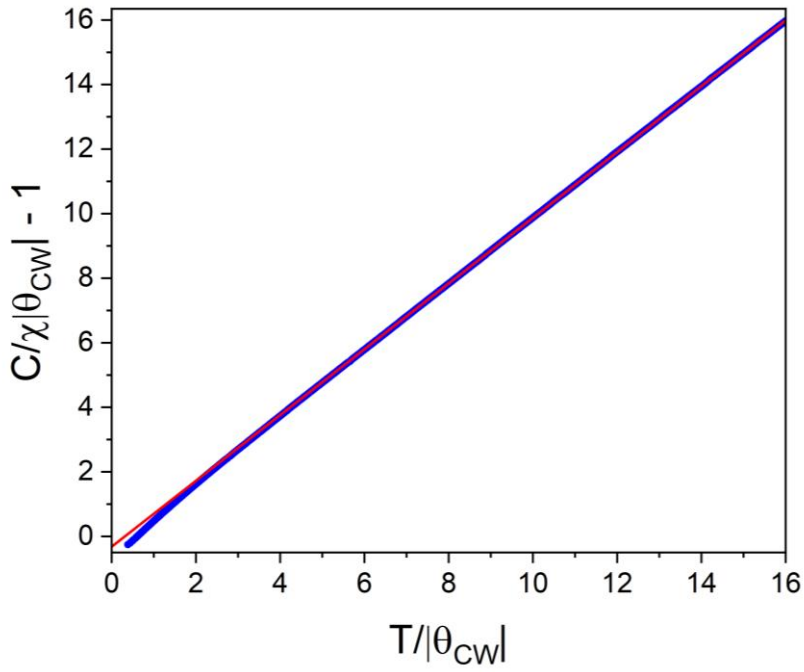

Fig. S21: Plot of $C/\chi|\theta_{CW}| - 1$ as a function of $T/|\theta_{CW}|$ for $Tb(HCO_2)(C_2O_4)$.

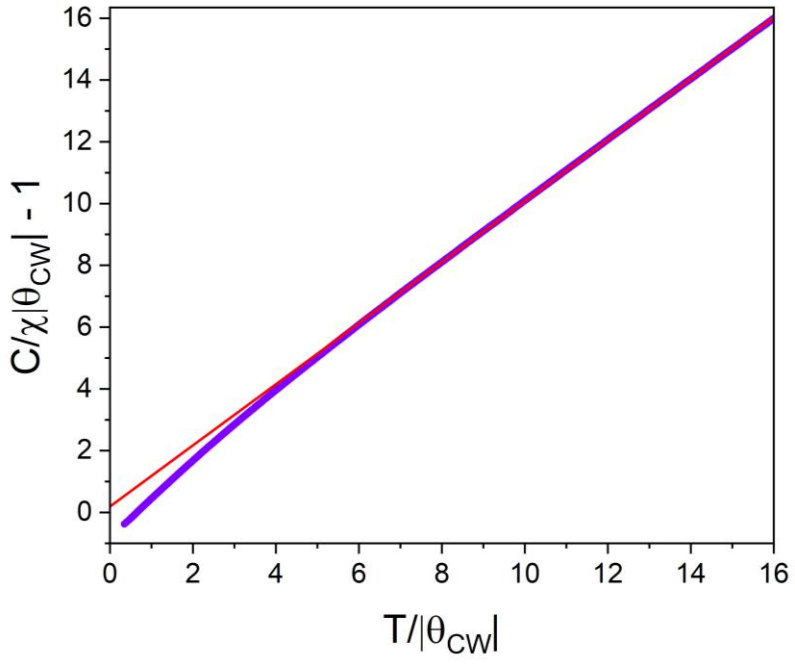

Fig. S22: Plot of $C/\chi|\theta_{CW}| - 1$ as a function of $T/|\theta_{CW}|$ for $Dy(HCO_2)(C_2O_4)$.

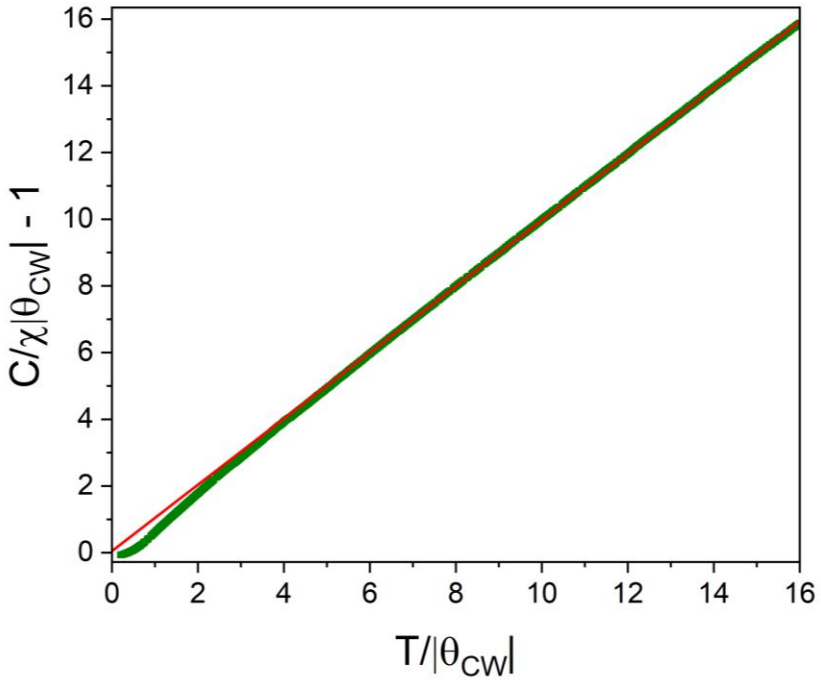

Fig. S23: Plot of $C/\chi|\theta_{CW}| - 1$ as a function of $T/|\theta_{CW}|$ for $Ho(HCO_2)(C_2O_4)$.

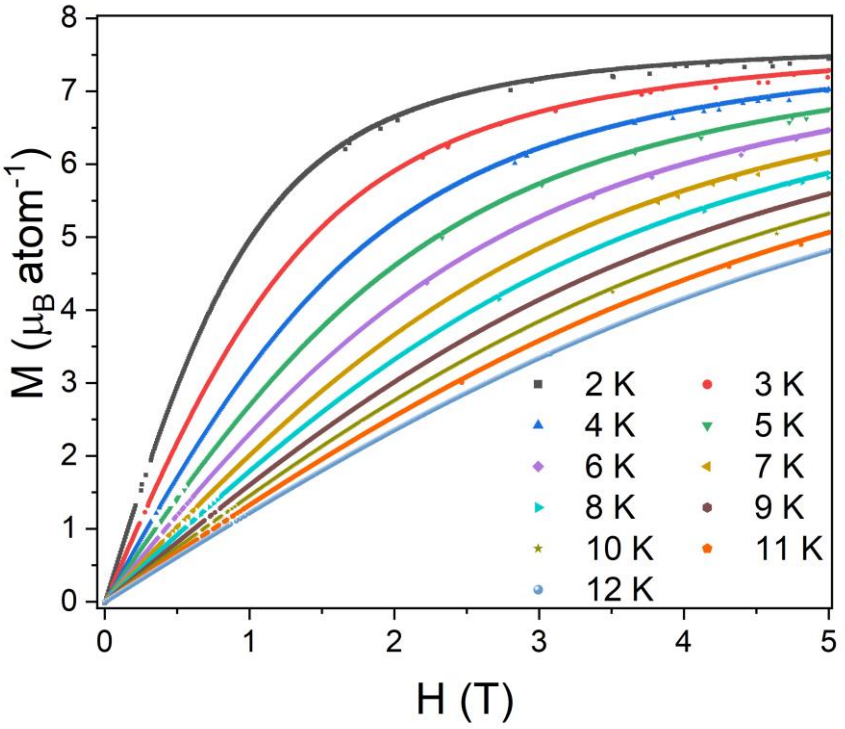

Fig. S24: Isothermal magnetisation measurements $Gd(HCO_2)(C_2O_4)$.

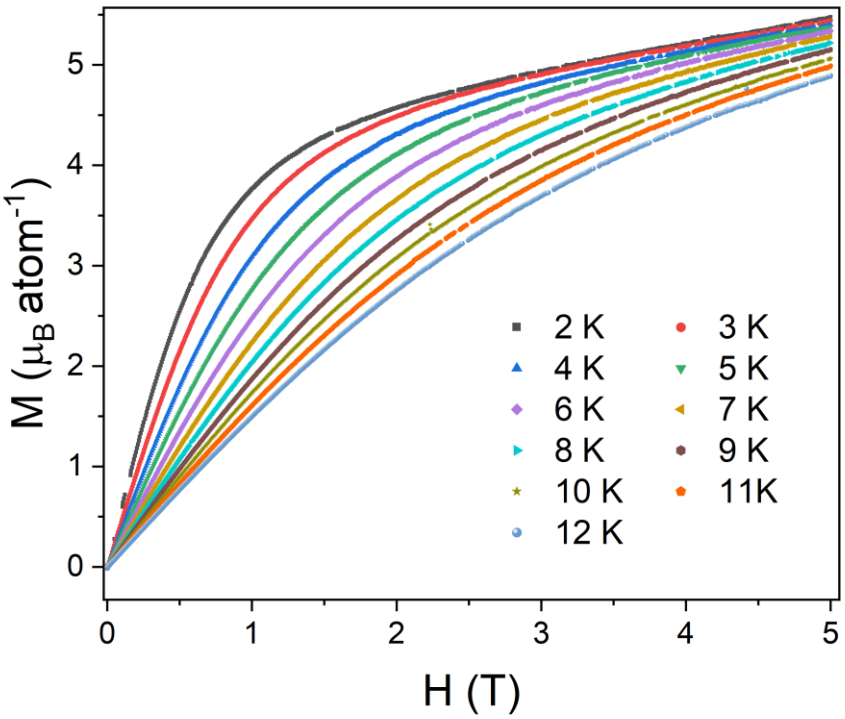

Fig. S25: Isothermal magnetisation measurements for $Tb(HCO_2)(C_2O_4)$.

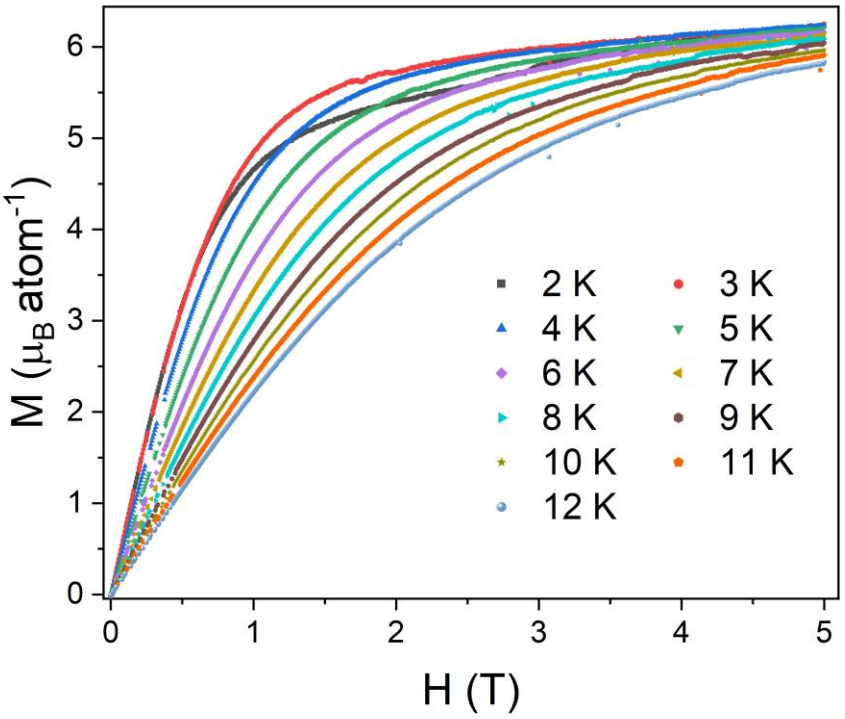

Fig. S26: Isothermal magnetisation measurements for $Dy(HCO_2)(C_2O_4)$.

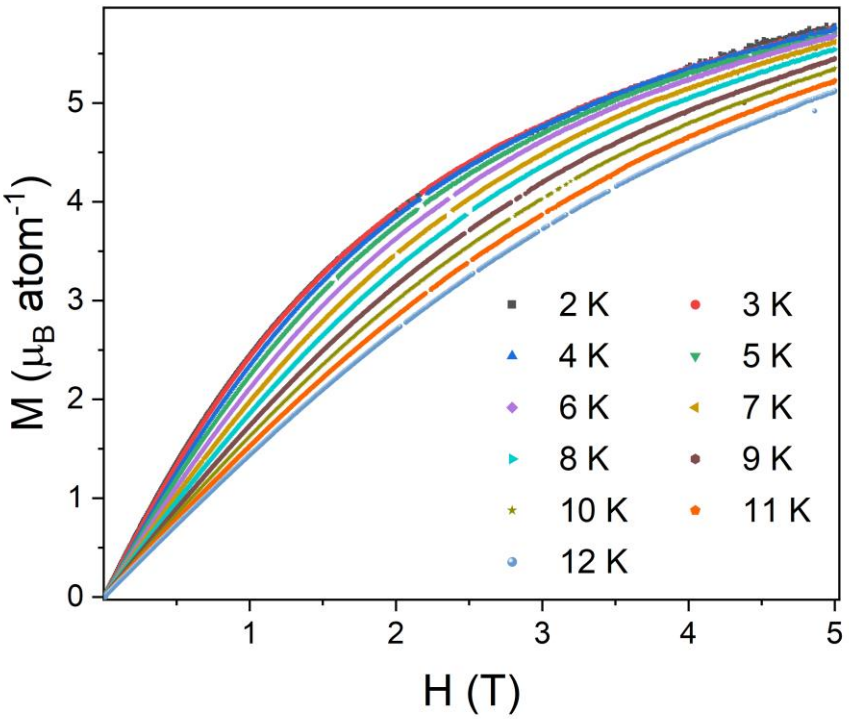

Fig. S27: Isothermal magnetisation measurements for $Ho(HCO_2)(C_2O_4)$.

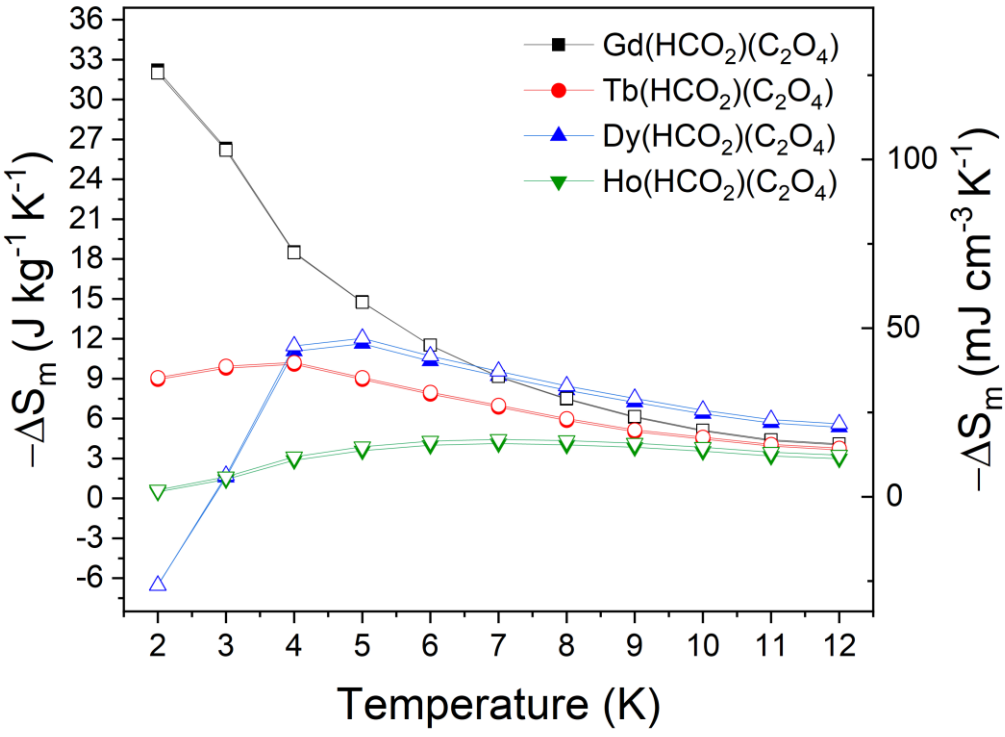

Fig. S28: Magnetic entropy changes for the $Ln(HCO_2)(C_2O_4)$ series for ΔB = 0-2 T. The filled and hollow symbols mark the gravimetric and volumetric units, respectively.

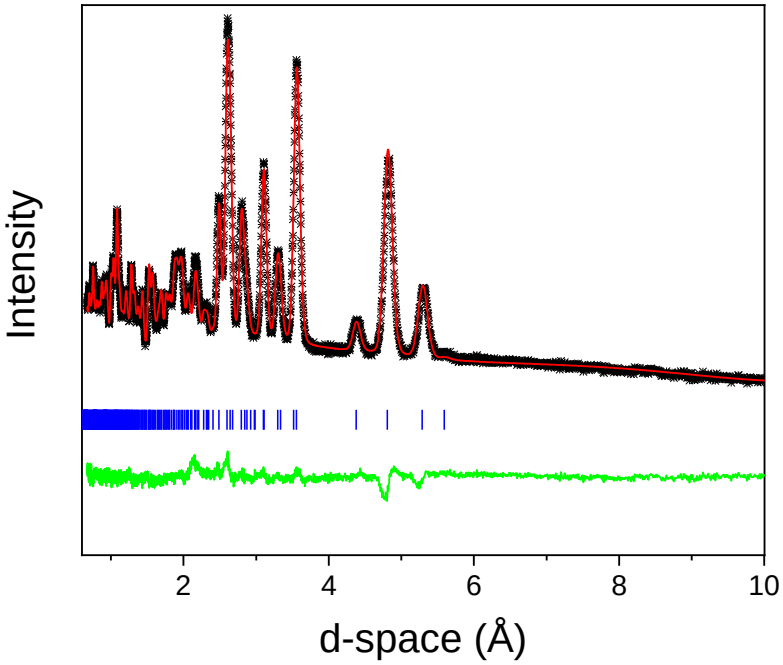

Fig. S29: Neutron diffraction pattern collected from $Tb(HCO_2)(C_2O_4)$ at room temperature using bank 2 of the GEM diffractometer fitted using the Rietveld method with R_p and R_{wp} of 2.67 % and 3.16 %, respectively. The crosses, upper and lower lines indicate the observed and calculated intensities and the differences between them. The markers indicate the reflection allowed by the structure.

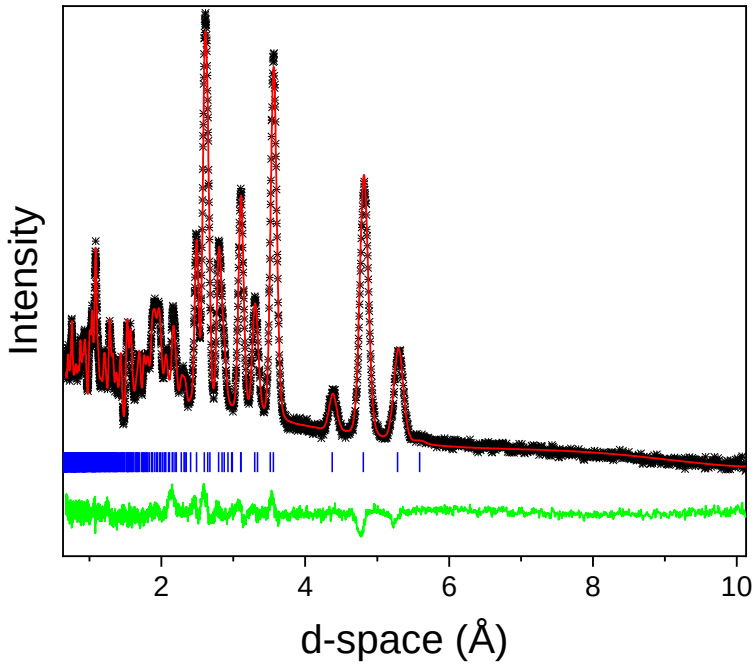

Fig. S30: Neutron diffraction pattern collected from $Tb(HCO_2)(C_2O_4)$ at 20 K using bank 2 of the GEM diffractometer fitted using the Rietveld method with R_p and R_{wp} of 1.65 % and 1.90 %, respectively. The crosses, upper and lower lines indicate the observed and calculated intensities and the differences between them. The markers indicate the reflection allowed by the structure.

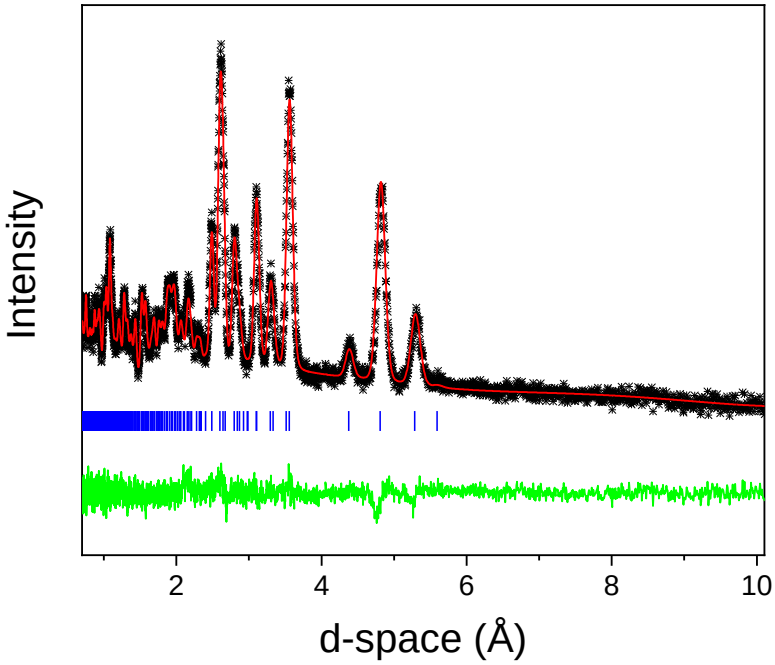

Fig. S31: Neutron diffraction pattern collected from $Tb(HCO_2)(C_2O_4)$ at 15 K using bank 2 of the GEM diffractometer fitted using the Rietveld method with R_p and R_{wp} of 2.47 % and 2.81 %, respectively. The crosses, upper and lower lines indicate the observed and calculated intensities and the differences between them. The markers indicate the reflection allowed by the structure.

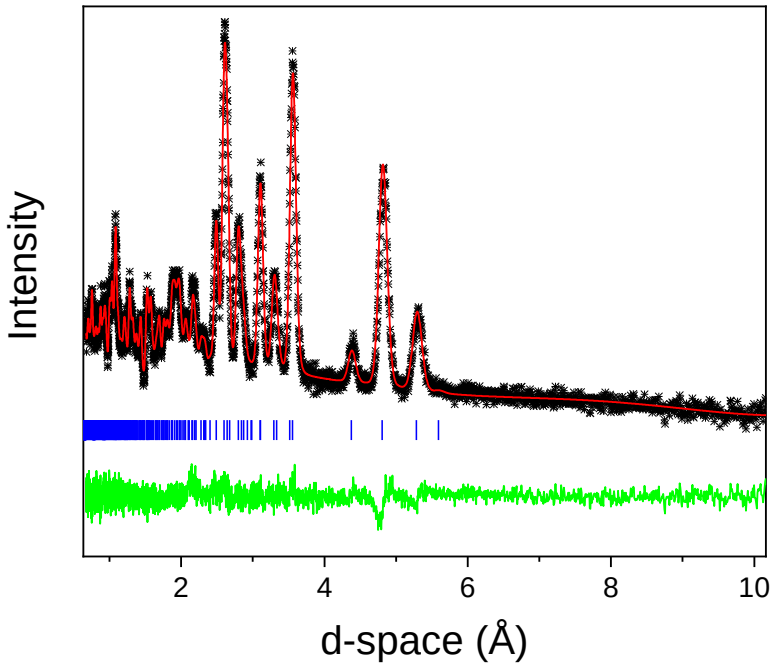

Fig. S32: Neutron diffraction pattern collected from $Tb(HCO_2)(C_2O_4)$ at 10 K using bank 2 of the GEM diffractometer fitted using the Rietveld method with R_p and R_{wp} of 2.45 % and 2.76 %, respectively. The crosses, upper and lower lines indicate the observed and calculated intensities and the differences between them. The markers indicate the reflection allowed by the structure.

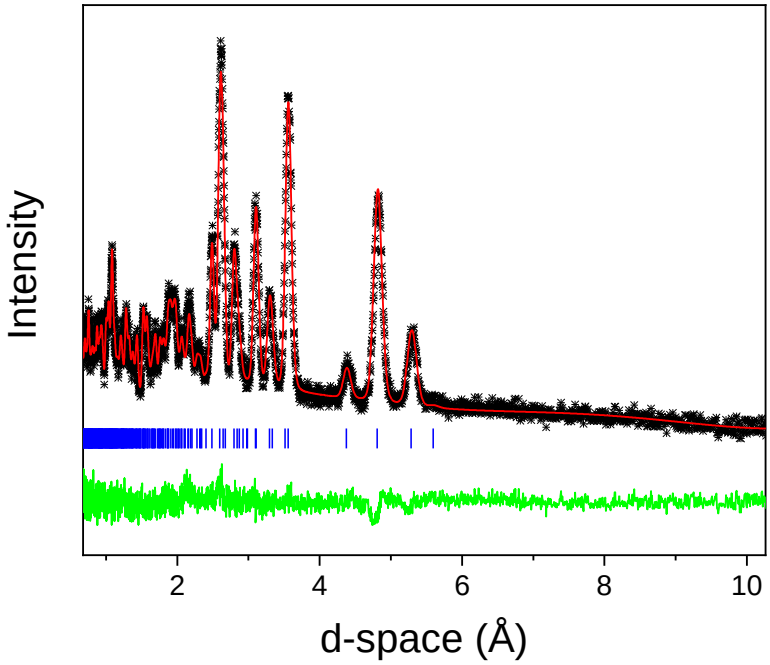

Fig. S33: Neutron diffraction pattern collected from $Tb(HCO_2)(C_2O_4)$ at 7 K using bank 2 of the GEM diffractometer fitted using the Rietveld method with R_p and R_{wp} of 2.43 % and 2.77 %, respectively. The crosses, upper and lower lines indicate the observed and calculated intensities and the differences between them. The markers indicate the reflection allowed by the structure.

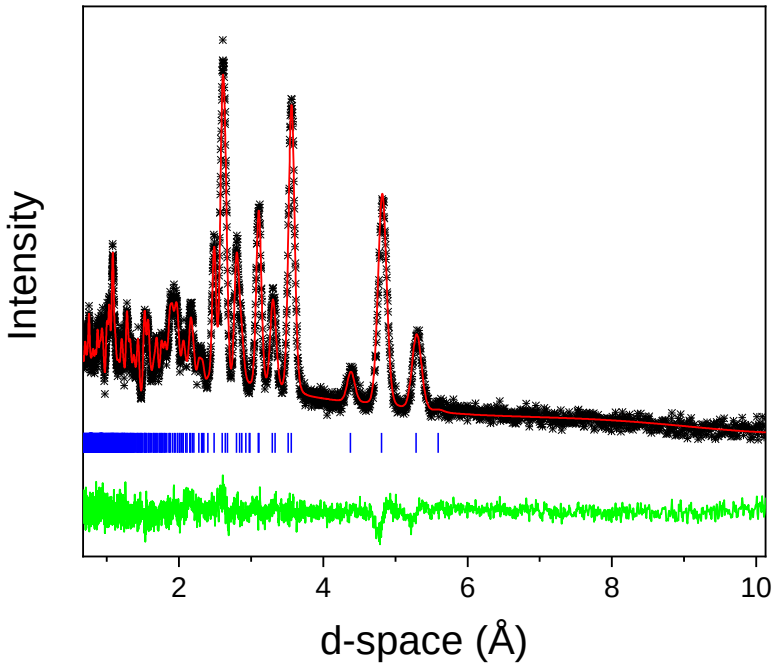

Fig. S34: Neutron diffraction pattern collected from $Tb(HCO_2)(C_2O_4)$ at 5 K using bank 2 of the GEM diffractometer fitted using the Rietveld method with R_p and R_{wp} of 2.52 % and 2.80 %, respectively. The crosses, upper and lower lines indicate the observed and calculated intensities and the differences between them. The markers indicate the reflection allowed by the structure.

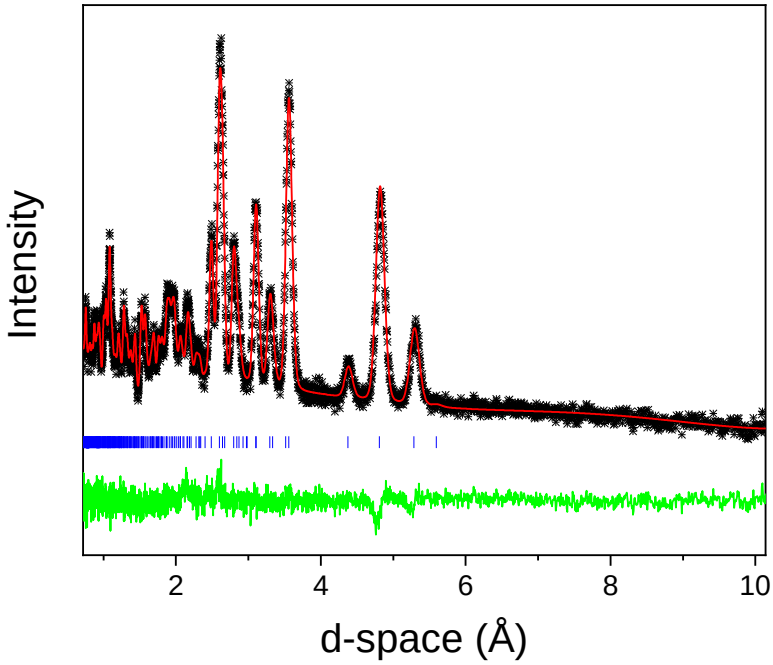

Fig. S35: Neutron diffraction pattern collected from $Tb(HCO_2)(C_2O_4)$ at 3 K using bank 2 of the GEM diffractometer fitted using the Rietveld method with R_p and R_{wp} of 2.41 % and 2.76 %, respectively. The crosses, upper and lower lines indicate the observed and calculated intensities and the differences between them. The markers indicate the reflection allowed by the structure.

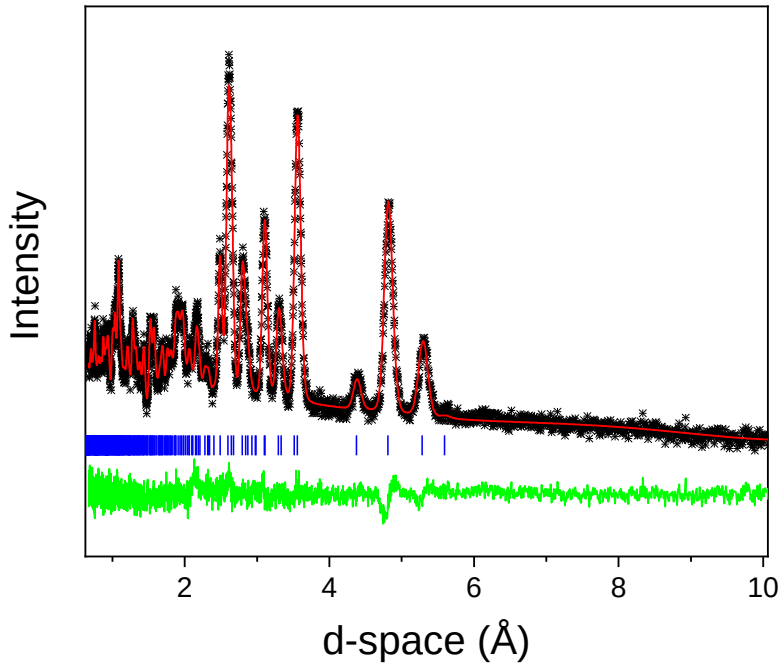

Fig. S36: Neutron diffraction pattern collected from $Tb(HCO_2)(C_2O_4)$ at 2.5 K using bank 2 of the GEM diffractometer fitted using the Rietveld method with R_p and R_{wp} of 2.49 % and 2.81 %, respectively. The crosses, upper and lower lines indicate the observed and calculated intensities and the differences between them. The markers indicate the reflection allowed by the structure.

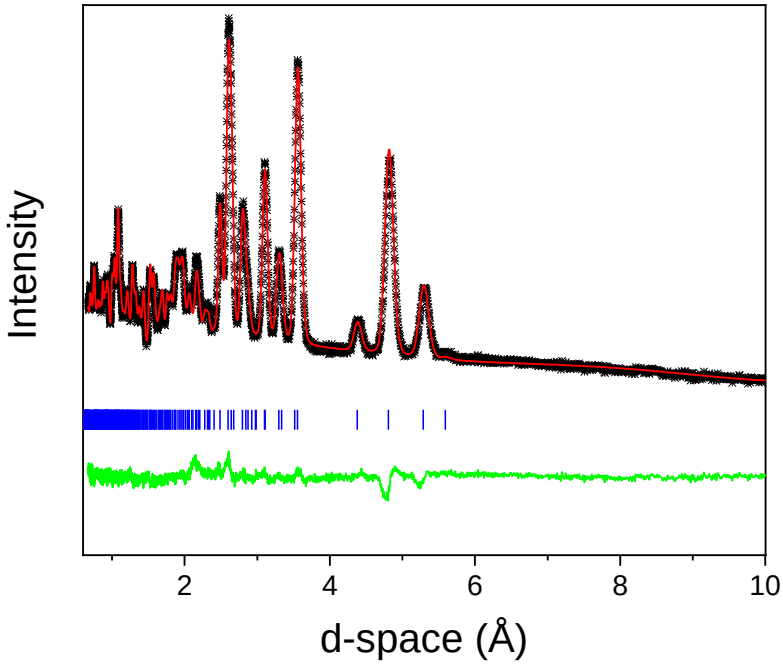

Fig. S37: Neutron diffraction pattern collected from $Tb(HCO_2)(C_2O_4)$ at 1.6 K using bank 2 of the GEM diffractometer fitted using the Rietveld method with R_p and R_{wp} of 1.55 % and 1.79 %, respectively. The crosses, upper and lower lines indicate the observed and calculated intensities and the differences between them. The markers indicate the reflection allowed by the structure.

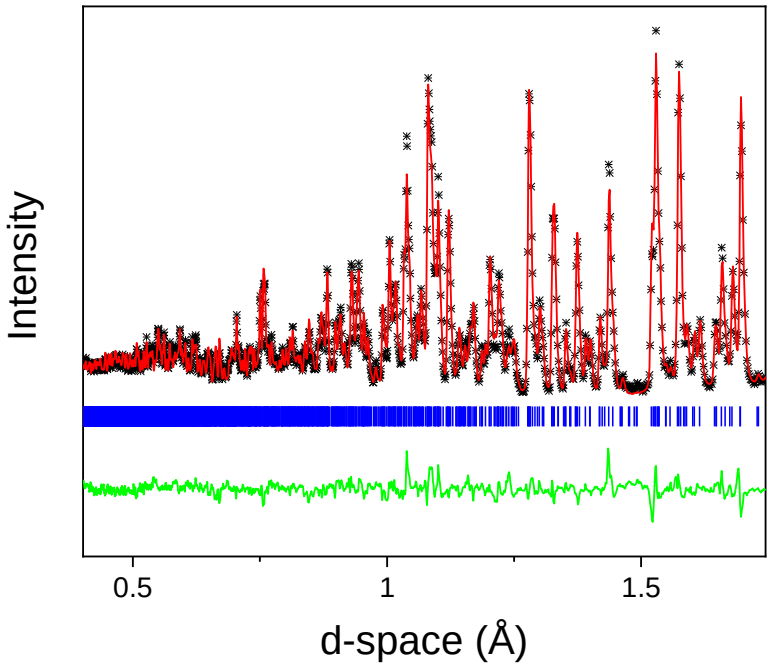

Fig. S38: Neutron diffraction pattern collected from $Tb(HCO_2)(C_2O_4)$ at room temperature using bank 6 of the GEM diffractometer fitted using the Rietveld method with R_p and R_{wp} of 2.67 % and 3.28%, respectively. The crosses, upper and lower lines indicate the observed and calculated intensities and the differences between them. The markers indicate the reflection allowed by the structure.

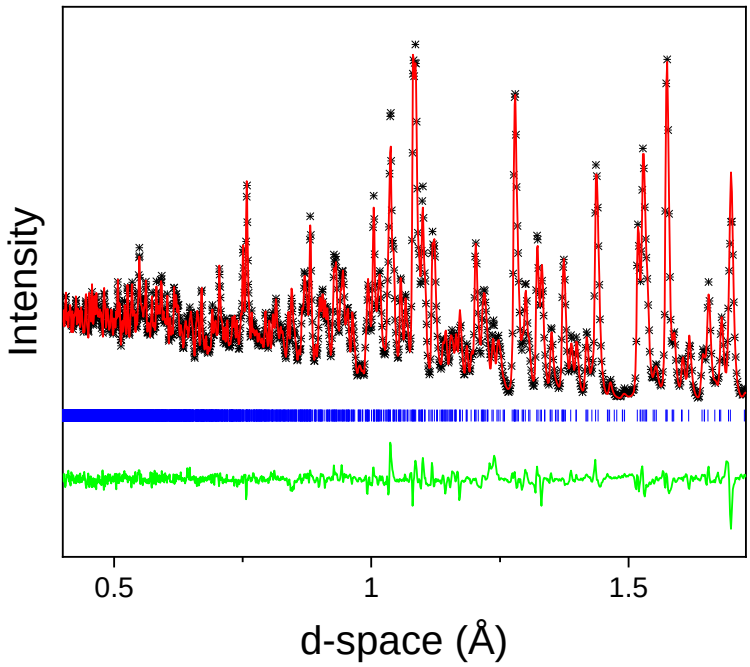

Fig. S39: Neutron diffraction pattern collected from $Tb(HCO_2)(C_2O_4)$ at 20 K using bank 6 of the GEM diffractometer fitted using the Rietveld method with R_p and R_{wp} of 1.81 % and 2.25 %, respectively. The crosses, upper and lower lines indicate the observed and calculated intensities and the differences between them. The markers indicate the reflection allowed by the structure.

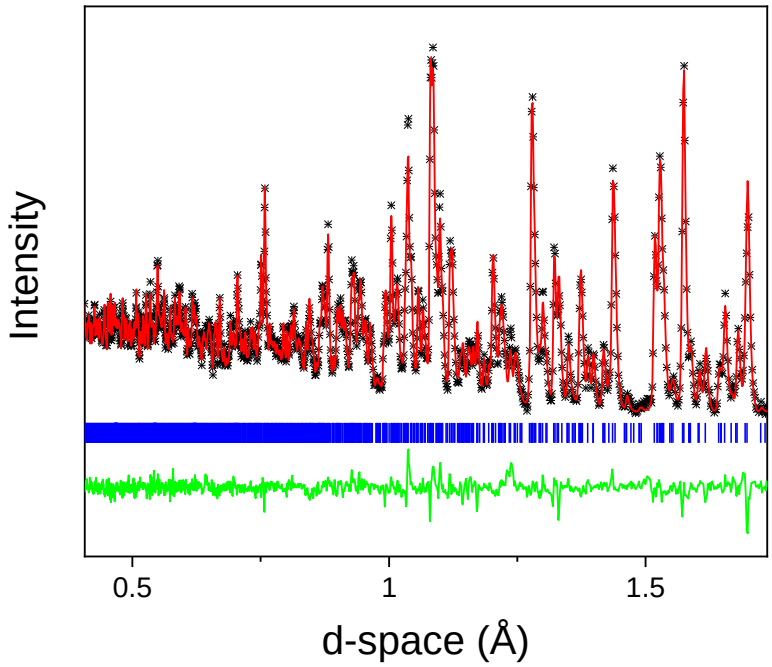

Fig. S40: Neutron diffraction pattern collected from $Tb(HCO_2)(C_2O_4)$ at 15 K using bank 6 of the GEM diffractometer fitted using the Rietveld method with R_p and R_{wp} of 1.73 % and 2.18 %, respectively. The crosses, upper and lower lines indicate the observed and calculated intensities and the differences between them. The markers indicate the reflection allowed by the structure.

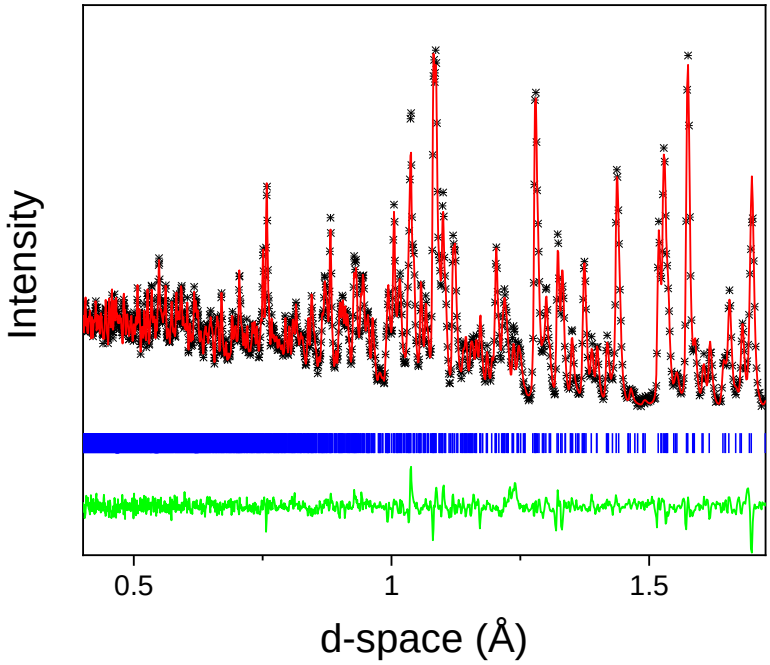

Fig. S41: Neutron diffraction pattern collected from $Tb(HCO_2)(C_2O_4)$ at 10 K using bank 6 of the GEM diffractometer fitted using the Rietveld method with R_p and R_{wp} of 1.71 % and 2.15 %, respectively. The crosses, upper and lower lines indicate the observed and calculated intensities and the differences between them. The markers indicate the reflection allowed by the structure.

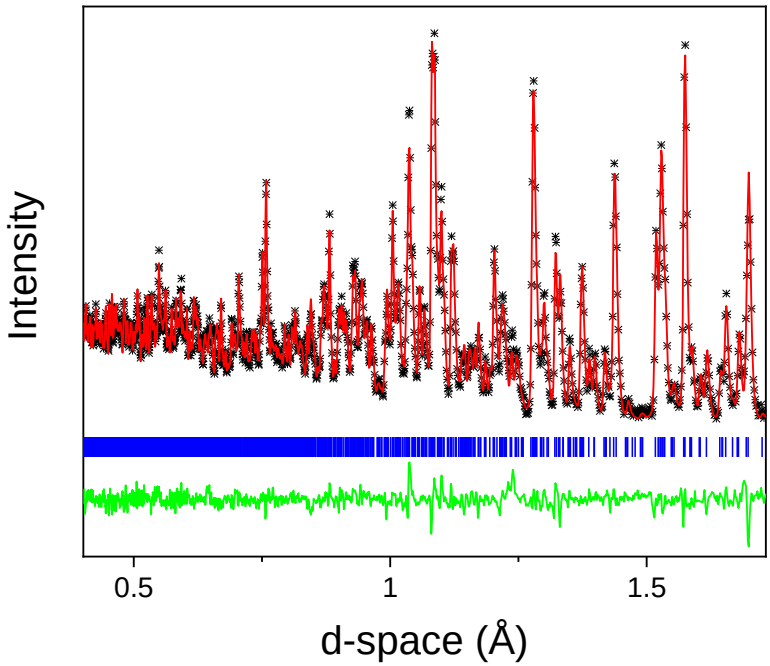

Fig. S42: Neutron diffraction pattern collected from $Tb(HCO_2)(C_2O_4)$ at 7 K using bank 6 of the GEM diffractometer fitted using the Rietveld method with R_p and R_{wp} of 1.71 % and 2.16 %, respectively. The crosses, upper and lower lines indicate the observed and calculated intensities and the differences between them. The markers indicate the reflection allowed by the structure.

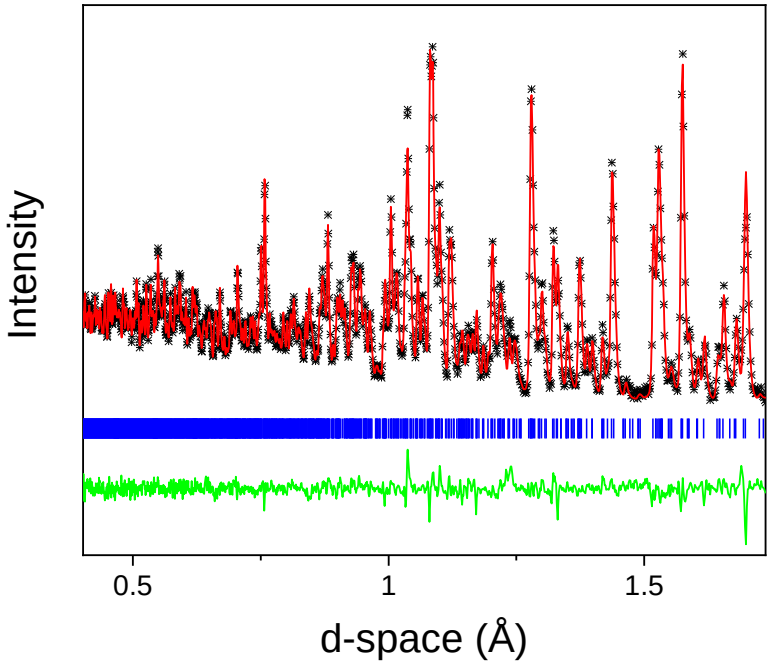

Fig. S43: Neutron diffraction pattern collected from $Tb(HCO_2)(C_2O_4)$ at 5 K using bank 6 of the GEM diffractometer fitted using the Rietveld method with R_p and R_{wp} of 1.72 % and 2.16 %, respectively. The crosses, upper and lower lines indicate the observed and calculated intensities and the differences between them. The markers indicate the reflection allowed by the structure.

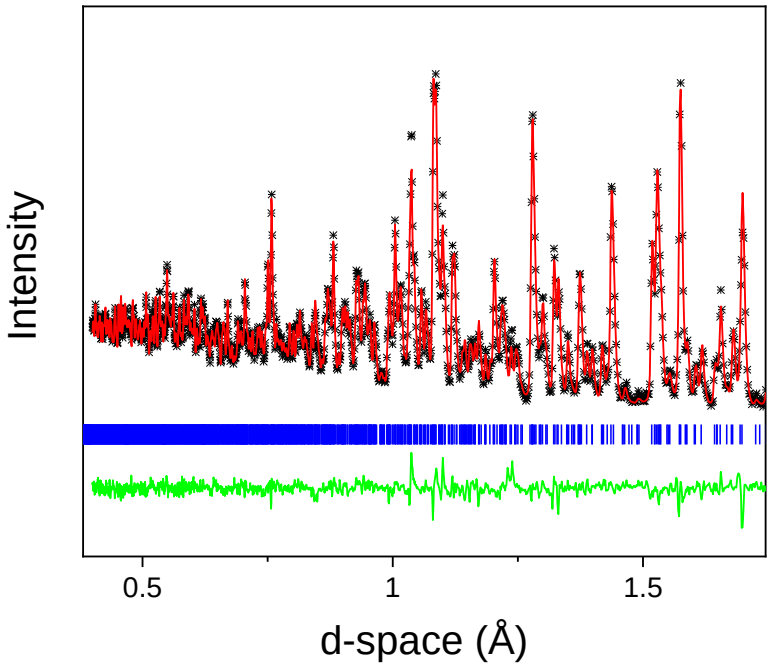

Fig. S44: Neutron diffraction pattern collected from $Tb(HCO_2)(C_2O_4)$ at 3 K using bank 6 of the GEM diffractometer fitted using the Rietveld method with R_p and R_{wp} of 1.68 % and 2.15 %, respectively. The crosses, upper and lower lines indicate the observed and calculated intensities and the differences between them. The markers indicate the reflection allowed by the structure.

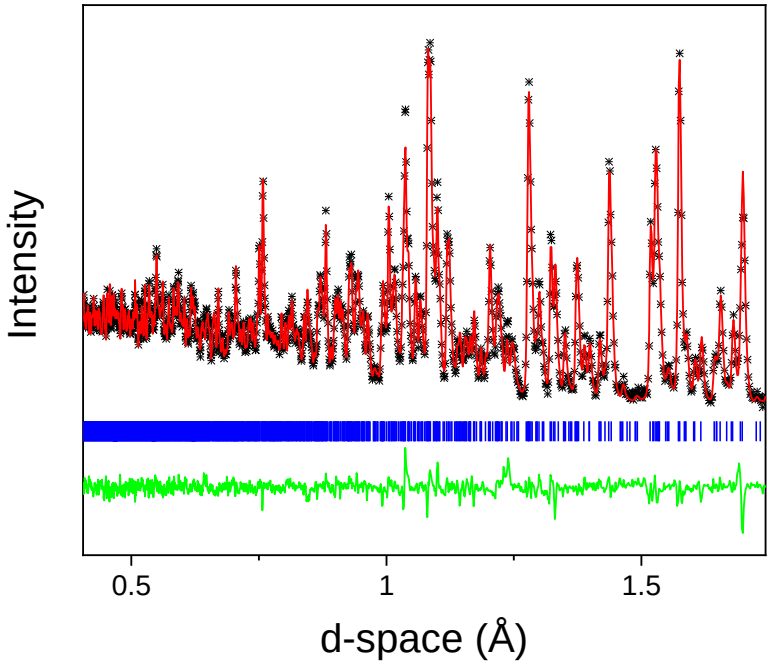

Fig. S45: Neutron diffraction pattern collected from $Tb(HCO_2)(C_2O_4)$ at 2.5 K using bank 6 of the GEM diffractometer fitted using the Rietveld method with R_p and R_{wp} of 1.67 % and 2.16 %, respectively. The crosses, upper and lower lines indicate the observed and calculated intensities and the differences between them. The markers indicate the reflection allowed by the structure.

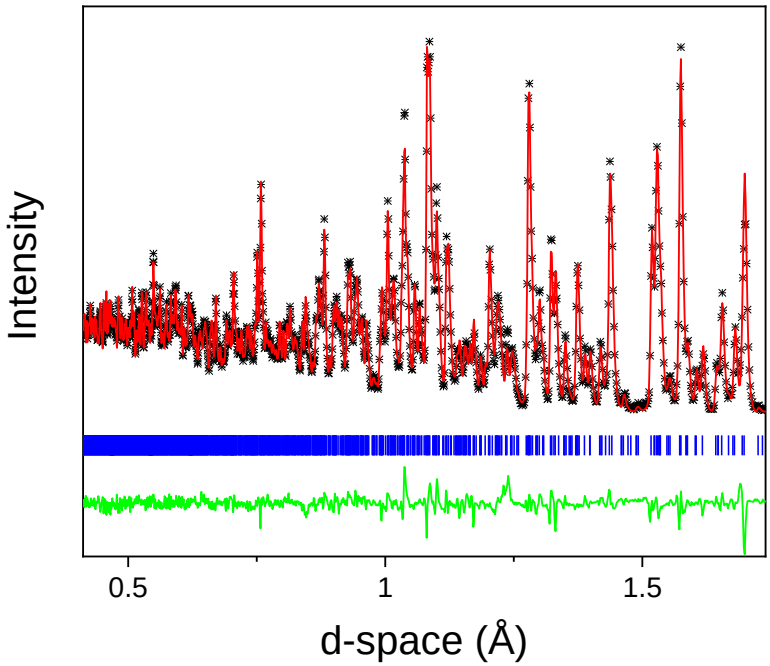

Fig. S46: Neutron diffraction pattern collected from $Tb(HCO_2)(C_2O_4)$ at 1.6 K using bank 6 of the GEM diffractometer fitted using the Rietveld method with R_p and R_{wp} of 1.48 % and 1.94 %, respectively. The crosses, upper and lower lines indicate the observed and calculated intensities and the differences between them. The markers indicate the reflection allowed by the structure.

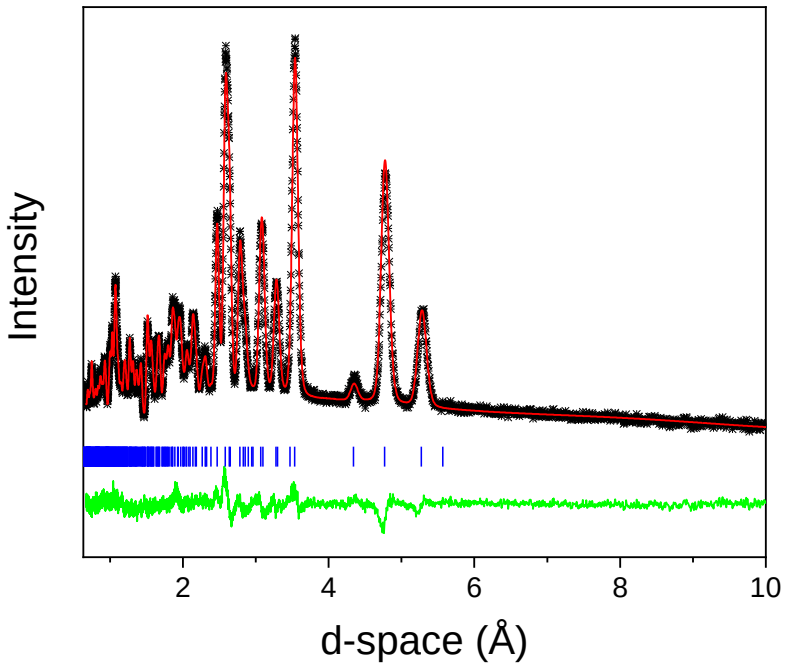

Fig. S47: Neutron diffraction pattern collected from $Ho(HCO_2)(C_2O_4)$ at room temperature using bank 2 of the GEM diffractometer fitted using the Rietveld method with R_p and R_{wp} of 2.61 % and 3.22 %, respectively. The crosses, upper and lower lines indicate the observed and calculated intensities and the differences between them. The markers indicate the reflection allowed by the structure.

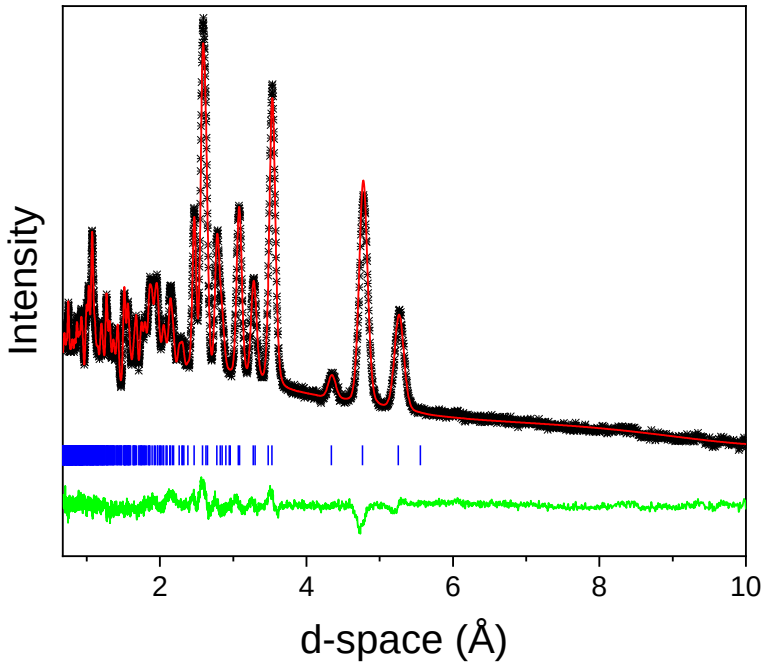

Fig. S48: Neutron diffraction pattern collected from $Ho(HCO_2)(C_2O_4)$ at 20 K using bank 2 of the GEM diffractometer fitted using the Rietveld method with R_p and R_{wp} of 1.65 % and 1.85 %, respectively. The crosses, upper and lower lines indicate the observed and calculated intensities and the differences between them. The markers indicate the reflection allowed by the structure.

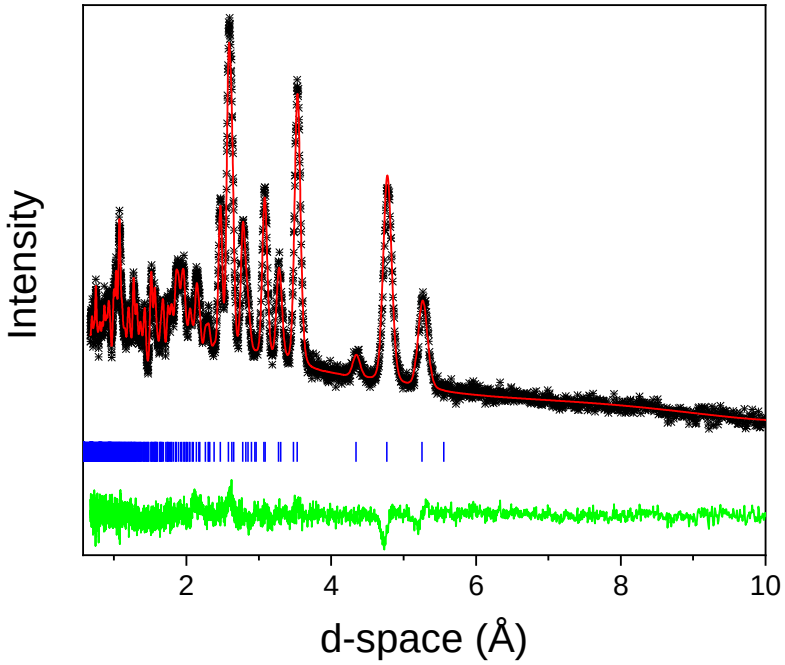

Fig. S49: Neutron diffraction pattern collected from $Ho(HCO_2)(C_2O_4)$ at 15 K using bank 2 of the GEM diffractometer fitted using the Rietveld method with R_p and R_{wp} of 2.55 % and 2.86 %, respectively. The crosses, upper and lower lines indicate the observed and calculated intensities and the differences between them. The markers indicate the reflection allowed by the structure.

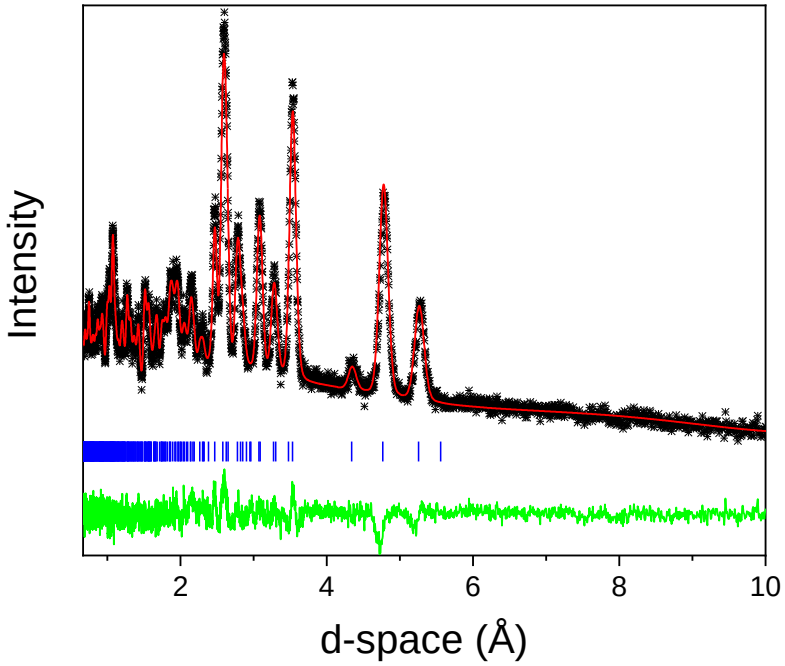

Fig. S50: Neutron diffraction pattern collected from $Ho(HCO_2)(C_2O_4)$ at 10 K using bank 2 of the GEM diffractometer fitted using the Rietveld method with R_p and R_{wp} of 2.63 % and 3.12 %, respectively. The crosses, upper and lower lines indicate the observed and calculated intensities and the differences between them. The markers indicate the reflection allowed by the structure.

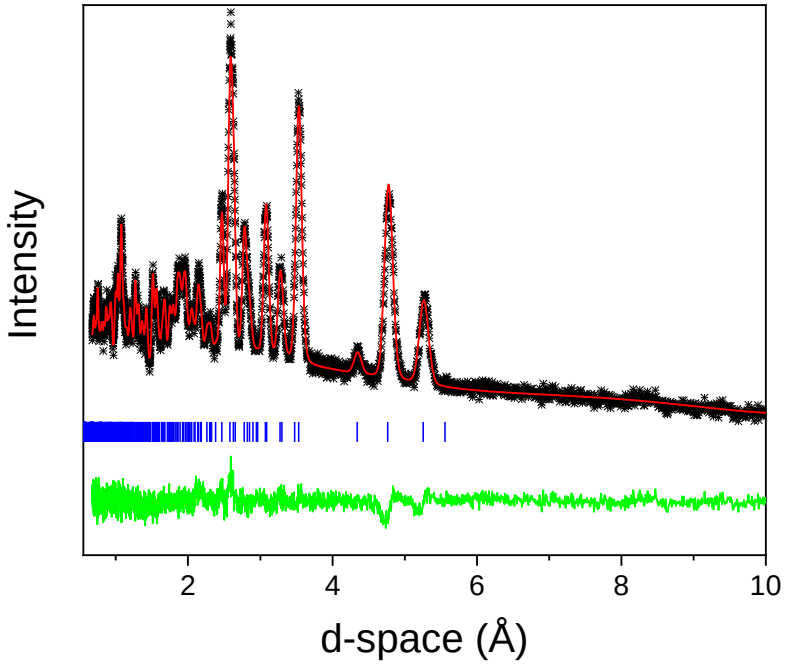

Fig. S51: Neutron diffraction pattern collected from $Ho(HCO_2)(C_2O_4)$ at 7 K using bank 2 of the GEM diffractometer fitted using the Rietveld method with R_p and R_{wp} of 2.55 % and 2.87 %, respectively. The crosses, upper and lower lines indicate the observed and calculated intensities and the differences between them. The markers indicate the reflection allowed by the structure.

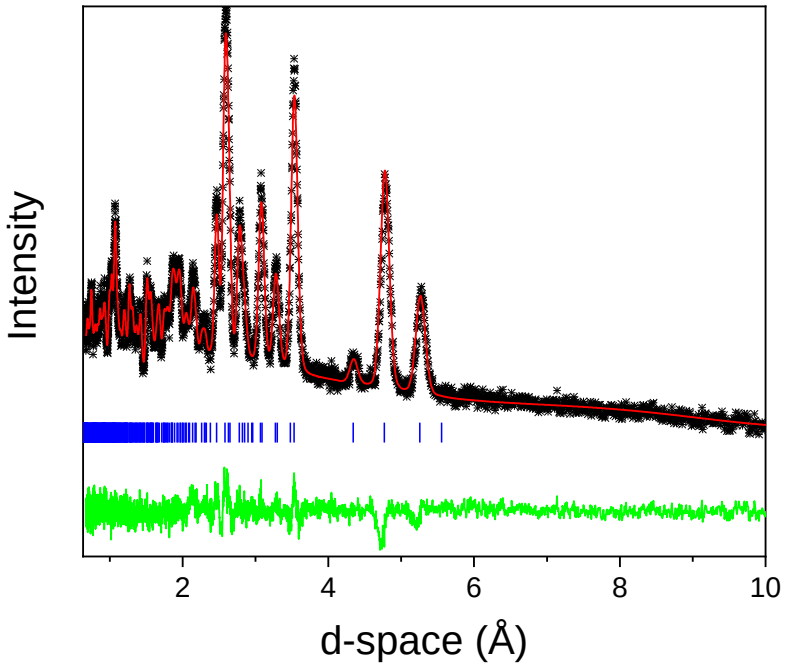

Fig. S52: Neutron diffraction pattern collected from $Ho(HCO_2)(C_2O_4)$ at 5 K using bank 2 of the GEM diffractometer fitted using the Rietveld method with R_p and R_{wp} of 2.71 % and 3.05 %, respectively. The crosses, upper and lower lines indicate the observed and calculated intensities and the differences between them. The markers indicate the reflection allowed by the structure.

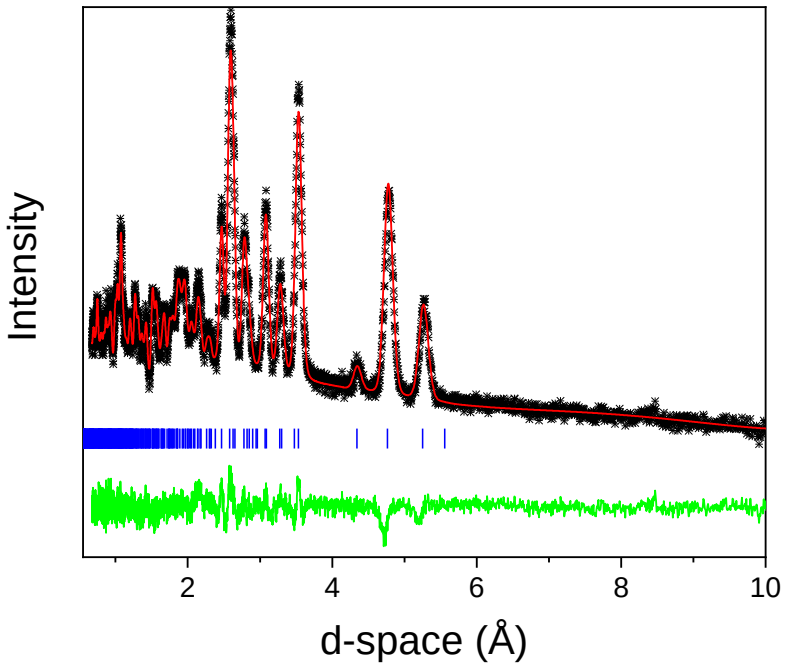

Fig. S53: Neutron diffraction pattern collected from $Ho(HCO_2)(C_2O_4)$ at 3 K using bank 2 of the GEM diffractometer fitted using the Rietveld method with R_p and R_{wp} of 2.55 % and 3.04 %, respectively. The crosses, upper and lower lines indicate the observed and calculated intensities and the differences between them. The markers indicate the reflection allowed by the structure.

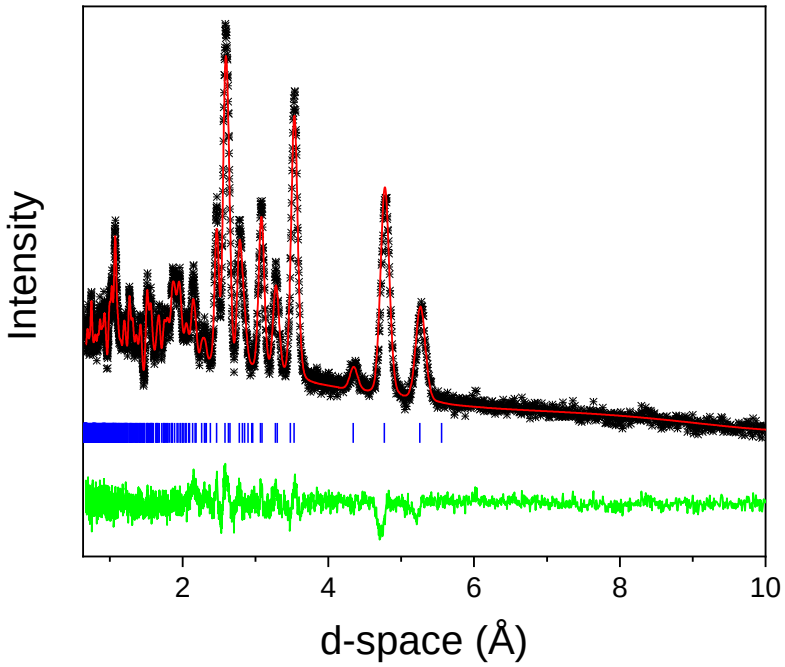

Fig. S54: Neutron diffraction pattern collected from $Ho(HCO_2)(C_2O_4)$ at 2.5 K using bank 2 of the GEM diffractometer fitted using the Rietveld method with R_p and R_{wp} of 2.57 % and 3.05 %, respectively. The crosses, upper and lower lines indicate the observed and calculated intensities and the differences between them. The markers indicate the reflection allowed by the structure.

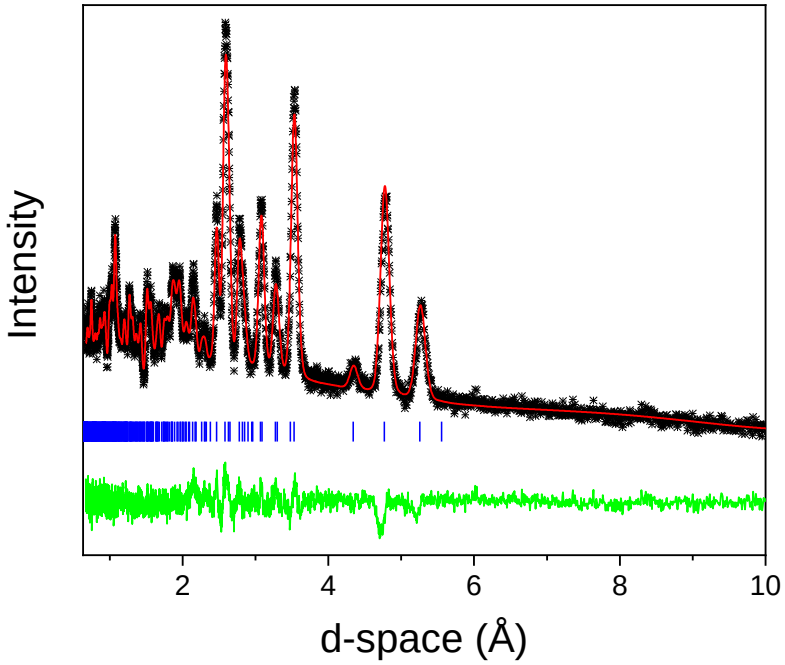

Fig. S55: Neutron diffraction pattern collected from $Ho(HCO_2)(C_2O_4)$ at 1.6 K using bank 2 of the GEM diffractometer fitted using the Rietveld method with R_p and R_{wp} of 1.56 % and 1.85 %, respectively. The crosses, upper and lower lines indicate the observed and calculated intensities and the differences between them. The markers indicate the reflection allowed by the structure.

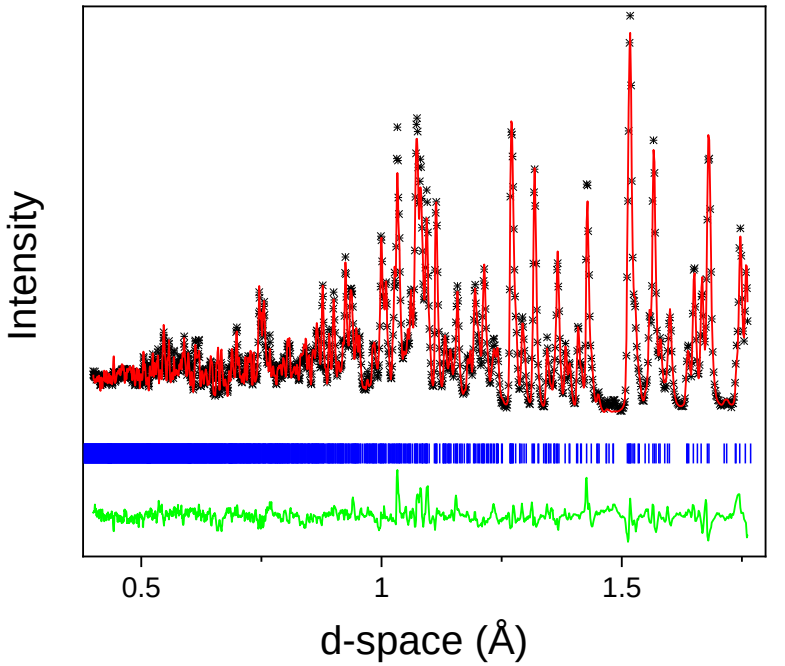

Fig. S56: Neutron diffraction pattern collected from $Ho(HCO_2)(C_2O_4)$ at room temperature using bank 6 of the GEM diffractometer fitted using the Rietveld method with R_p and R_{wp} of 2.65 % and 3.25 %, respectively. The crosses, upper and lower lines indicate the observed and calculated intensities and the differences between them. The markers indicate the reflection allowed by the structure.

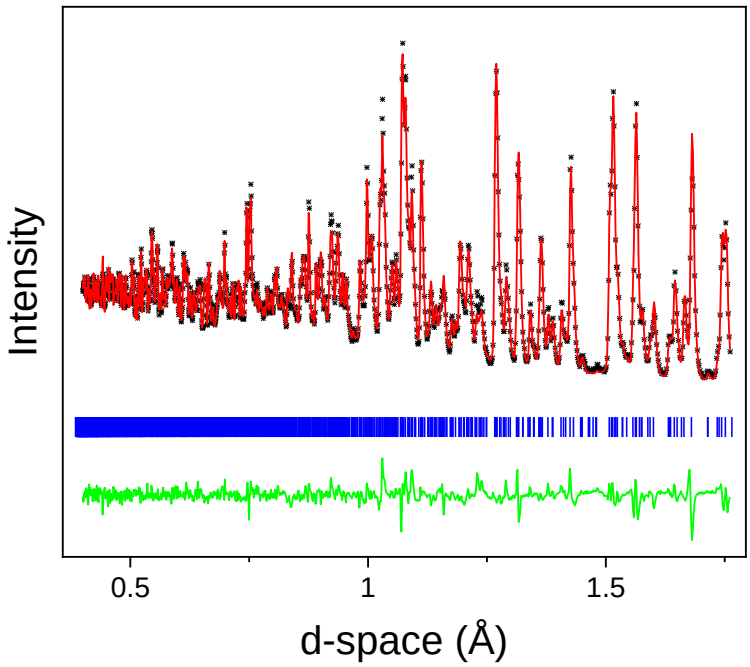

Fig. S57: Neutron diffraction pattern collected from $Ho(HCO_2)(C_2O_4)$ at 20 K using bank 6 of the GEM diffractometer fitted using the Rietveld method with R_p and R_{wp} of 1.69 % and 2.1 %, respectively. The crosses, upper and lower lines indicate the observed and calculated intensities and the differences between them. The markers indicate the reflection allowed by the structure.

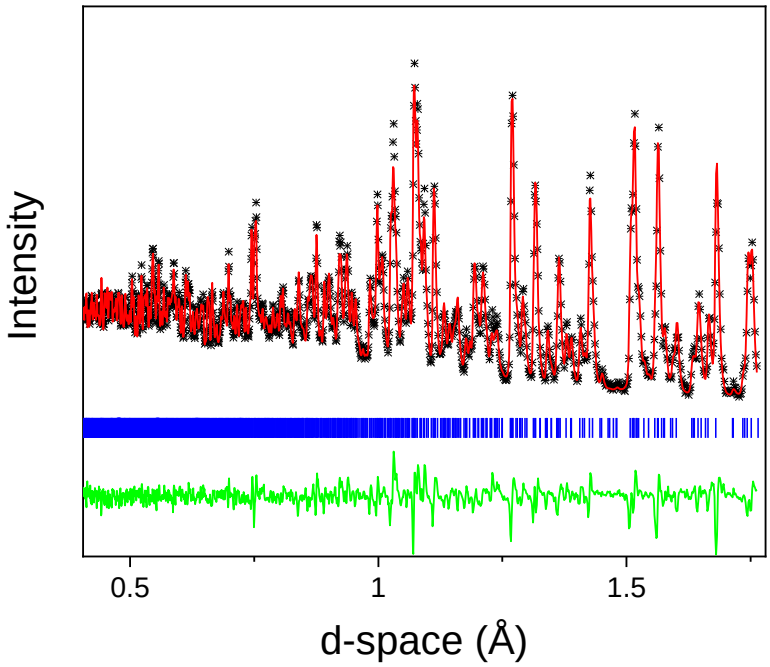

Fig. S58: Neutron diffraction pattern collected from $Ho(HCO_2)(C_2O_4)$ at 15 K using bank 6 of the GEM diffractometer fitted using the Rietveld method with R_p and R_{wp} of 2.50 % and 3.19 %, respectively. The crosses, upper and lower lines indicate the observed and calculated intensities and the differences between them. The markers indicate the reflection allowed by the structure.

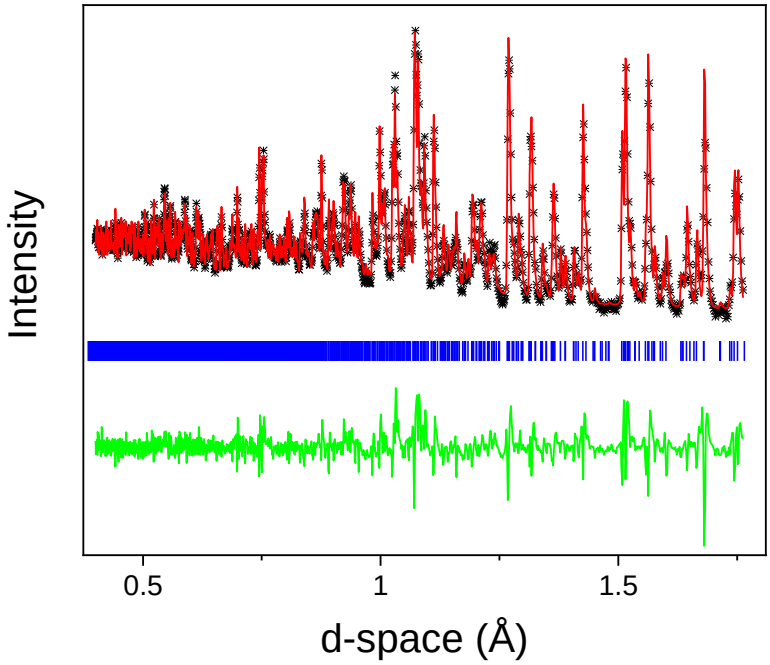

Fig. S59: Neutron diffraction pattern collected from $Ho(HCO_2)(C_2O_4)$ at 10 K using bank 6 of the GEM diffractometer fitted using the Rietveld method with R_p and R_{wp} of 3.66 % and 4.59 %, respectively. The crosses, upper and lower lines indicate the observed and calculated intensities and the differences between them. The markers indicate the reflection allowed by the structure.

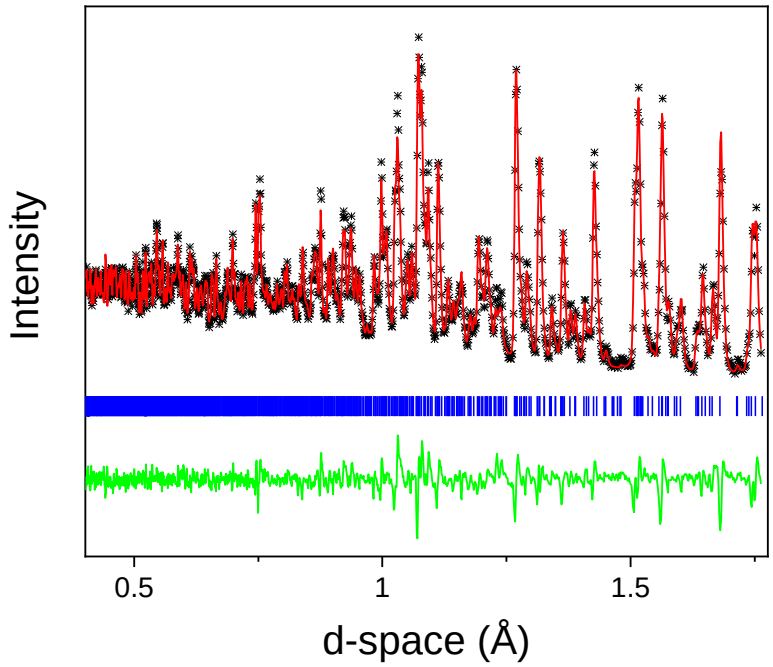

Fig. S60: Neutron diffraction pattern collected from $Ho(HCO_2)(C_2O_4)$ at 7 K using bank 6 of the GEM diffractometer fitted using the Rietveld method with R_p and R_{wp} of 2.47 % and 3.16 %, respectively. The crosses, upper and lower lines indicate the observed and calculated intensities and the differences between them. The markers indicate the reflection allowed by the structure.

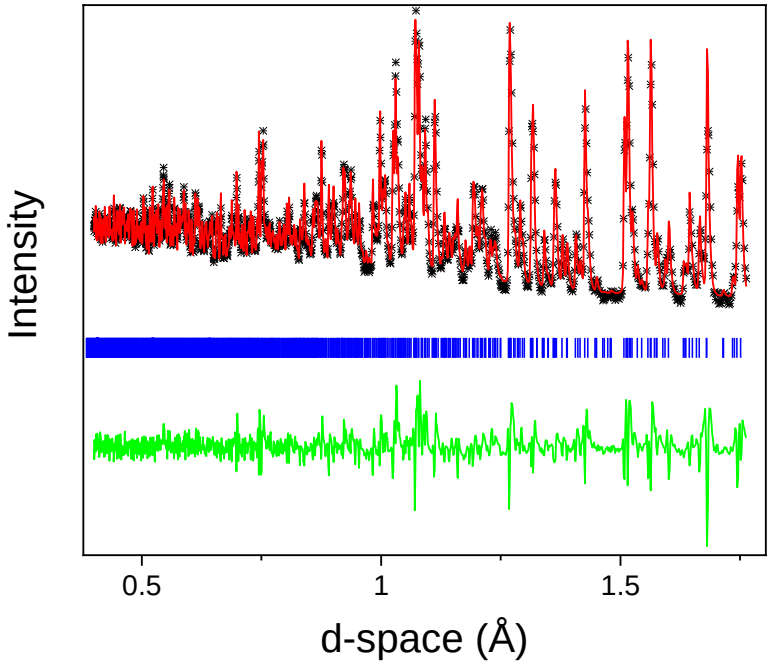

Fig. S61: Neutron diffraction pattern collected from $Ho(HCO_2)(C_2O_4)$ at 5 K using bank 6 of the GEM diffractometer fitted using the Rietveld method with R_p and R_{wp} of 3.80 % and 4.73 %, respectively. The crosses, upper and lower lines indicate the observed and calculated intensities and the differences between them. The markers indicate the reflection allowed by the structure.

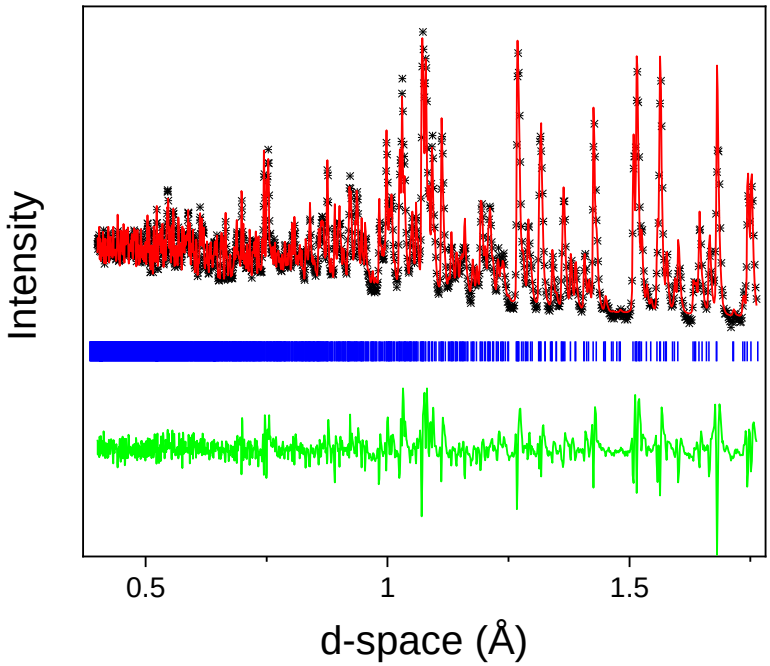

Fig. S62: Neutron diffraction pattern collected from $Ho(HCO_2)(C_2O_4)$ at 3 K using bank 6 of the GEM diffractometer fitted using the Rietveld method with R_p and R_{wp} of 3.84 % and 4.78 %, respectively. The crosses, upper and lower lines indicate the observed and calculated intensities and the differences between them. The markers indicate the reflection allowed by the structure.

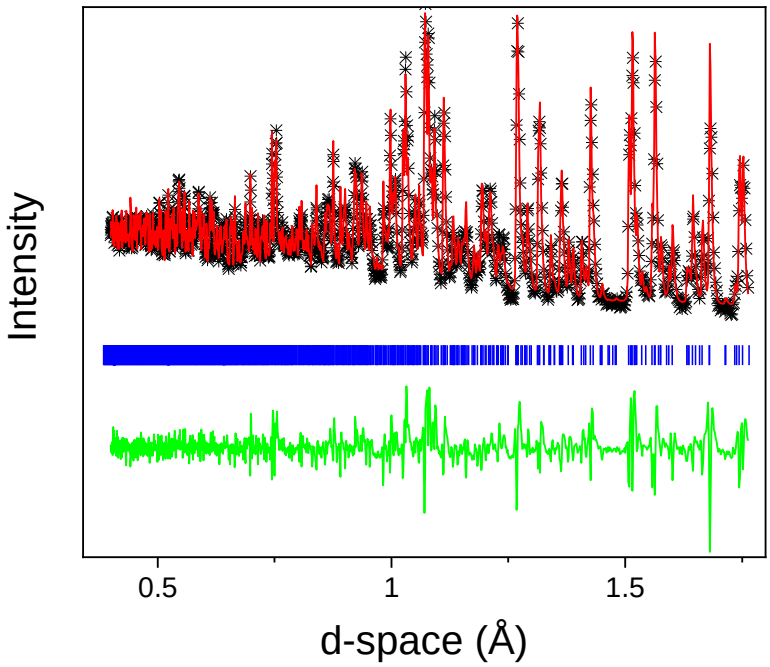

Fig. S63: Neutron diffraction pattern collected from $Ho(HCO_2)(C_2O_4)$ at 2.5 K using bank 6 of the GEM diffractometer fitted using the Rietveld method with R_p and R_{wp} of 3.76 % and 4.71 %, respectively. The crosses, upper and lower lines indicate the observed and calculated intensities and the differences between them. The markers indicate the reflection allowed by the structure.

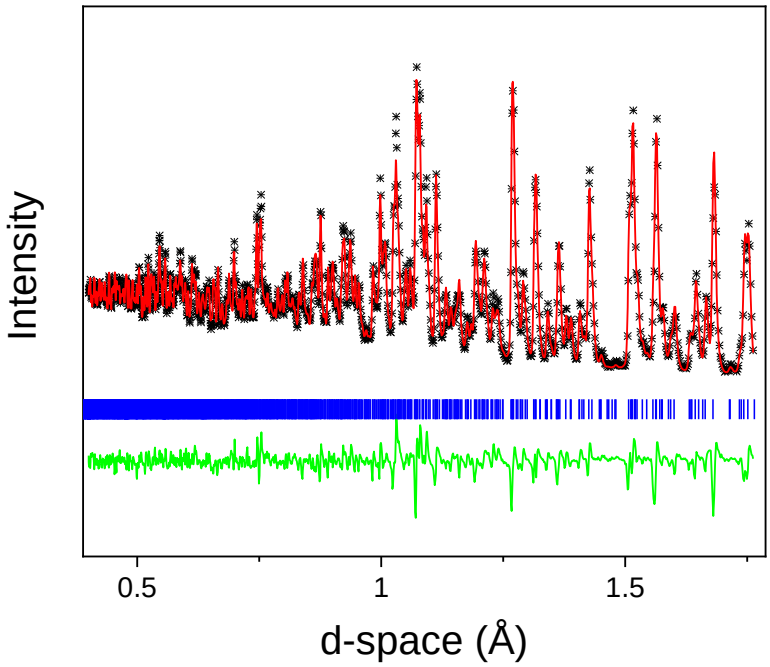

Fig. S64: Neutron diffraction pattern collected from $Ho(HCO_2)(C_2O_4)$ at 1.6 K using bank 6 of the GEM diffractometer fitted using the Rietveld method with R_p and R_{wp} of 2.38 % and 3.09 %, respectively. The crosses, upper and lower lines indicate the observed and calculated intensities and the differences between them. The markers indicate the reflection allowed by the structure.

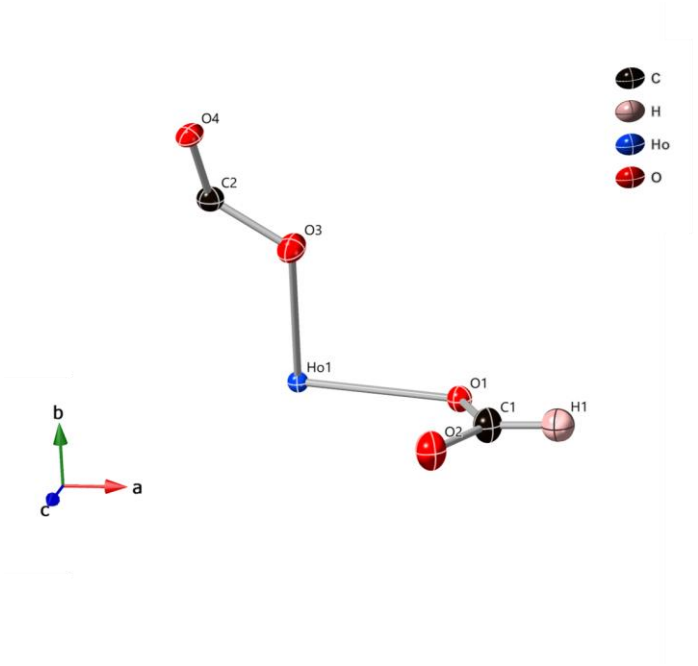

Fig. S65: Asymmetric unit of $Ho(HCO_2)(C_2O_4)$ with atoms shown as ellipsoids with a 60% probability for electron density.

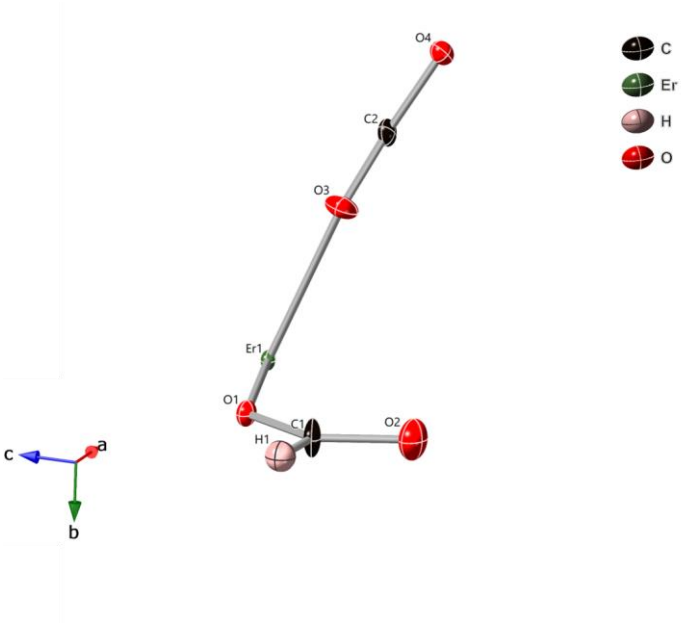

Fig. S66: Asymmetric unit of $Er(HCO_2)(C_2O_4)$ with atoms shown as ellipsoids with a 60% probability to find electron density.

Table S1: Selected bond distances for $Ho(HCO_2)(C_2O_4)$ collected at 120 K

	Distance (Å)
Ho1-O1	2.391(3)
Ho1-O1	2.451(3)
Ho1-O2	2.402(3)
Ho1-O3	2 x 2.390(2)
Ho1-O4	2 x 2.413(2)
Ho1-O4	2 x 2.437(2)
O1-C1	1.269(6)
O2-C1	1.228(6)
O3-C2	1.242(4)
O4-C2	1.261(4)

Table S2: Selected bond distances for $Er(HCO_2)(C_2O_4)$ collected at 120 K.

	Distance (Å)
Er1-O1	2.379(4)
Er1-O1	2.439(4)
Er1-O2	2.386(4)
Er1-O3	2 x 2.380(3)
Er1-O4	2 x 2.406(3)
Er1-O4	2 x 2.422(3)
O1-C1	1.279(7)
O2-C1	1.225(8)
O3-C2	1.239(5)
O4-C2	1.269(5)

Table S3: Crystallographic details of $Tb(HCO_2)(C_2O_4)$ obtained from neutron diffraction patterns collected at 300 K. Final total refinement statistics R_p and R_{wp} were 2.88 % and 3.27 %, respectively.

Space Group	*a* (Å)	*b* (Å)	*c* (Å)	Volume (Å^3)	
Pnma	7.01686(13)	10.59776(21)	6.59239(12)	490.230(23)	
Site	x	Y	z	U_{iso}(Å^2)	Fractional Occupancy
Tb	0.20348	3/4	0.63422	0.00153(18)	1
O1	0.53263(18)	3/4	0.53803(22)	0.00531(31)	1
O2	0.55264(26)	3/4	0.19929(21)	0.0131(4)	1
O3	0.23803(15)	0.54453(9)	0.47981(13)	0.00692(20)	1
O4	0.08552(13)	0.37694(8)	0.35167(16)	0.00640(20)	1
C1	0.61900(21)	3/4	0.37264(22)	0.01240(31)	1
C2	0.09644(13)	0.47884(7)	0.45248(11)	0.00331(17)	1
D	0.77114(29)	3/4	0.37656(32)	0.0681(7)	1

Table S4: Crystallographic details of $Tb(HCO_2)(C_2O_4)$ obtained from neutron diffraction patterns collected at 20 K. Final total refinement statistics R_p and R_{wp} were 2.02 % and 2.79 %, respectively.

Space Group	*a* (Å)	*b* (Å)	*c* (Å)	Volume (Å^3)	
Pnma	7.02827(12)	10.56945(18)	6.59041(11)	489.569(20)	
Site	x	Y	z	U_{iso}(Å^2)	Fractional Occupancy
Tb	0.20348	3/4	0.64422	-0.00154(14)	1
O1	0.53581(15)	3/4	0.53670(19)	-0.00129(21)	1
O2	0.55371(21)	3/4	0.19622(18)	0.00347(26)	1
O3	0.23952(13)	0.54446(8)	0.48093(12)	0.00219(16)	1
O4	0.08759(12)	0.37633(8)	0.34904(15)	0.00139(16)	1
C1	0.62361(15)	3/4	0.37314(18)	-0.00040(19)	1
C2	0.09602(12)	0.47884(6)	0.45179(11)	0.0079(14)	1
D	0.77928(20)	3/4	0.37937(23)	0.0193(5)	1

Table S5: Crystallographic details of $Tb(HCO_2)(C_2O_4)$ obtained from neutron diffraction patterns collected at 1.6 K. Final total refinement statistics R_p and R_{wp} were 1.78 % and 2.33 %, respectively.

Space Group	*a* (Å)	*b* (Å)	*c* (Å)	Volume (Å^3)	
Pnma	7.02786(7)	10.56956(9)	6.59095(6)	489.585(5)	
Site	x	y	z	U_{iso}(Å^2)	Fractional Occupancy
Tb	0.20348	3/4	0.63422	-0.00226(11)	1
O1	0.53412(13)	3/4	0.53750(16)	-0.00014(18)	1
O2	0.55451(17)	3/4	0.19809(15)	0.00273(20)	1
O3	0.23976(11)	0.54461(7)	0.48073(10)	0.00123(12)	1
O4	0.08744(10)	0.37650(6)	0.35105(12)	0.00055(12)	1
C1	0.62398(13)	3/4	0.37206(16)	0.00114(17)	1
C2	0.09633(10)	0.47893(5)	0.45247(9)	0.00007(11)	1
D	0.77909(17)	3/4	0.37732(20)	0.02200(32)	1

Table S6: Crystallographic details of $Ho(HCO_2)(C_2O_4)$ obtained from neutron diffraction patterns collected at 300 K. Final total refinement statistics R_p and R_{wp} were 2.88 % and 3.31 %, respectively.

Space Group	*a* (Å)	*b* (Å)	*c* (Å)	Volume (Å^3)	
Pnma	6.94353(14)	10.54245(21)	6.55458(13)	479.807(24)	
Site	x	Y	z	U_{iso}(Å^2)	Fractional Occupancy
Ho	0.20113	¼	0.36659	-0.00065(16)	1
O1	0.08687(14)	0.62422(9)	0.64978(17)	0.00554(14)	1
O2	0.24041(15)	0.45462(10)	0.52007(14)	0.00554(14)	1
O3	0.55174(26)	¼	0.80239(22)	0.00782(2)	1
O4	0.53045(21)	¼	0.46186(25)	0.00782(2)	1
C1	0.09750(14)	0.52095(8)	0.54864(13)	0.00507(15)	1
C2	0.61799(21)	¼	0.62692(22)	0.00507(15)	1
D	0.77263(32)	¼	0.6240(4)	0.0725(8)	1

Table S7: Crystallographic details of $Ho(HCO_2)(C_2O_4)$ obtained from neutron diffraction patterns collected at 20 K. Final total refinement statistics R_p and R_{wp} were 2.00 % and 2.54 %, respectively.

Space Group	*a* (Å)	*b* (Å)	*c* (Å)	Volume (Å^3)	
Pnma	6.95296(11)	10.50898(17)	6.54600(10)	478.307(18)	
Site	x	Y	z	U_{iso}(Å^2)	Fractional Occupancy
Ho	0.20113	¼	0. 36659	-0.00362(10)	1
O1	0.08872(12)	0.62483(7)	0.64957(14)	0.00059(10)	1
O2	0.24191(12)	0.45439(8)	0.52021(12)	0.00059(10)	1
O3	0.55309(20)	1/4	0.80342(17)	0.00097(14)	1
O4	0.53296(16)	1/4	0.46215(19)	0.00097(14)	1
C1	0.09695(11)	0.52101(6)	0.54860(10)	-0.00021(10)	1
C2	0.62232(16)	1/4	0.62810(18)	-0.00021(10)	1
D	0.77998(20)	1/4	0.62224(24)	0.0241(4)	1

Table S8: Crystallographic details of $Ho(HCO_2)(C_2O_4)$ obtained from neutron diffraction patterns collected at 1.6 K. Final total refinement statistics R_p and R_{wp} were 2.11 % and 2.93 %, respectively.

Space Group	*a* (Å)	*b* (Å)	*c* (Å)	Volume (Å^3)	
Pnma	6.95346(9)	10.50704(12)	6.54620(7)	478.267(7)	
Site	x	y	z	U_{iso}(Å^2)	Fractional Occupancy
Ho	0.20113	1/4	0.36659	-0.00354(12)	1
O1	0.08872(13)	0.62480(8)	0.64964(16)	0.00052(11)	1
O2	0.24198(14)	0.45426(9)	0.52040(13)	0.00052(11)	1
O3	0.55321(23)	1/4	0.80343(20)	0.00102(16)	1
O4	0.53300(18)	1/4	0.46191(22)	0.00102(16)	1
C1	0.09696(13)	0.52098(7)	0.54850(12)	-0.000023(11)	1
C2	0.62227(18)	1/4	0.62787(21)	-0.000023(11)	1
D	0.78002(23)	1/4	0.62203(27)	0.0242(4)	1